Quaternary Science Reviews 346 (2024) 109053

Contents lists available at ScienceDirect

Quaternary Science Reviews

journal homepage: www.elsevier.com/locate/quascirev

Chronology of late Holocene relative sea-level change in Boston Harbor

Andrew C. Kemp *, Elaine M. Whetstine, John C. Ridge

Department of Earth and Climate Sciences, Tufts University, Medford, MA, 02155, USA

ARTICLE INFO

Handling Editor: Dr I Hendy

Keywords:
Salt marsh
Radiocarbon
Foraminifera
Bayesian transfer function

ABSTRACT

We use a core of salt-marsh sediment from Boston Harbor (Massachusetts, USA) to evaluate the sensitivity of late Holocene relative sea-level (RSL) reconstructions to the pre-treatment, graphitization, and upcore distribution of radiocarbon dates. The 87 radiocarbon dates from 58 unique depths in the 4.2-m long core show that ages from plant macrofossils (principally rhizomes and stems of *Spartina patens* and *Distichlis spicata*) are insensitive to pre-treatment and graphitization regimes. Statistical resampling from the pool of radiocarbon dates generated many plausible chronologies and demonstrates that the precision of age-depth models increases as dates are added, but with diminishing returns. Estimated sample ages are not systematically biased by the density of dates. Identification of periods with slower sedimentation requires a higher density of dates than identifying periods with faster sedimentation. These results suggest that RSL variability reconstructed among sites and regions is unlikely to be the result of choices in the preparation and selection of samples from salt-marsh sediment for radiocarbon dating. We reconstructed paleomarsh elevation using a Bayesian transfer function trained on the observed relationship between salt-marsh foraminifera and tidal elevation in 212 surface-sediment samples. This model utilized informative prior information from bulk-sediment $\delta^{13}C$ values. During the past ~4200 years RSL rose by ~4.2 m in Boston Harbor at a rate of ~0.9 mm/yr until the early 20th century when the rate increased to ~3 mm/yr, which is consistent with estimates of glacio-isostatic adjustment and historic tide-gauge measurements in Boston Harbor.

1. Introduction

Increasing frequency and severity of flooding driven by relative sea-level (RSL) rise is hazardous to the intense concentrations of socio-economic activity in coastal cities such as Boston (Martello and Whittle, 2023; Parsons et al., 2023; Strauss et al., 2015). Tide-gauge measurements show that RSL in Boston Harbor rose at ~2.6 mm/yr during the 20th century, having increased sharply at ~1920 CE (Ray and Foster, 2016; Talke et al., 2018). This rate of rise will accelerate during the remainder of the 21st century and beyond (DeConto et al., 2016). Proxy-based reconstructions of pre-anthropogenic RSL change provide a context for historic and predicted rates of rise (Gehrels et al., 2005; Walker et al., 2022), and insight into the causes and magnitude of natural sea-level variability on (multi-)century timescales (Gehrels et al., 2020; Walker et al., 2021). In regions that experienced sustained RSL rise during the late Holocene (such as the U.S. Atlantic coast), sediment that accumulated in salt marshes can yield detailed and near-continuous histories of RSL change (e.g., Stearns et al., 2023). These records are generated by building composite chronologies (radiocarbon and marker horizons of known age) to establish sedimentation histories using age-depth models (Wright et al., 2017) and using sea-level proxies such as foraminifera (Scott and Medioli, 1978), or bulk-sediment isotopic composition (Wilson et al., 2024) to establish the height of RSL. The Atlantic coast of North America has a relatively dense network of late Holocene RSL reconstructions (Walker et al., 2022), although a paucity of records in the Gulf of Maine hinders efforts to quantify and explain regional-scale sea-level variability. Salt marshes in Boston Harbor represent an opportunity to increase the density of records in the Gulf of Maine.

Broadly, the relationship between rates of sea-level change and sedimentation determines how salt-marsh stratigraphies record RSL. Disequilibrium of rates (if sufficiently large in magnitude and duration) causes drowning or emergence of the salt-marsh surface, which sea-level proxies record as temporal (upcore) variability, such as a shift in foraminifera to assemblages with different tolerances of tidal inundation. In these stratigraphies, RSL reconstructions rely on interpreting variability in the sea-level proxy and establishing a robust history of sedimentation. Equilibrium of rates causes the salt-marsh surface to maintain its

* Corresponding author.
E-mail address: andrew.kemp@tufts.edu (A.C. Kemp).

https://doi.org/10.1016/j.quascirev.2024.109053
Received 2 September 2024; Received in revised form 24 October 2024; Accepted 27 October 2024

elevation in the tidal frame, which sea-level proxies record by their stability (e.g., foraminiferal assemblages that do not change up core). Stratigraphies representing equilibrium are targeted for RSL reconstructions because the history of RSL change mirrors the history of sedimentation and is less dependent on (although not independent of) interpretation of sea-level proxies. Under such circumstances it is particularly important to understand how (in)sensitive age-depth models are to necessary sampling and analytical decisions made when building a chronology, such as the preparation, number, and within-core distribution of radiocarbon dates. Previous studies indicated that these choices are likely more influential than the decision of which specific age-depth model to adopt (Lacourse and Gajewski, 2020; Wright et al., 2017).

We use a core of salt-marsh sediment collected from Belle Isle Marsh in Boston Harbor (Fig. 1) to reconstruct RSL change during the past ~4200 years. A history of sediment accumulation is generated from 87 radiocarbon dates and recognition of three historic pollution and land-use changes of known age. The height of past sea-level is established using a multi-proxy approach, in which a Bayesian transfer function (generated from a modern training set of new and existing data) applied to preserved assemblages of foraminifera utilizes prior information about environment of deposition gleaned from upcore profiles of stable carbon isotopes ($\delta^{13}C$) in bulk sediment. The stratigraphy beneath Belle Isle Marsh (thick accumulations of high salt-marsh sediment accumulating at ~1 mm/yr) make it broadly representative of stratigraphies that are regularly used to reconstruct late Holocene RSL on the Atlantic coast of North America. Therefore, the resulting RSL reconstruction is used in three capacities. Firstly, we explore how radiocarbon dating of common salt-marsh macrofossils (predominantly rhizomes and stems of *Spartina patens* and *Distichlis spicata*) may be influenced by varied approaches to pre-treatment, graphitization, and measurement. Secondly, resampling of the unusually high density of radiocarbon dates in the core produces a large suite of chronologies that are representative of typical sampling strategies. Comparisons among these chronologies provides insight into how the number and within-core distribution of radiocarbon dates can influence RSL reconstructions. We do not compare results from different age-depth modeling software packages (Wright et al., 2017). Thirdly, the proxy reconstruction provides a

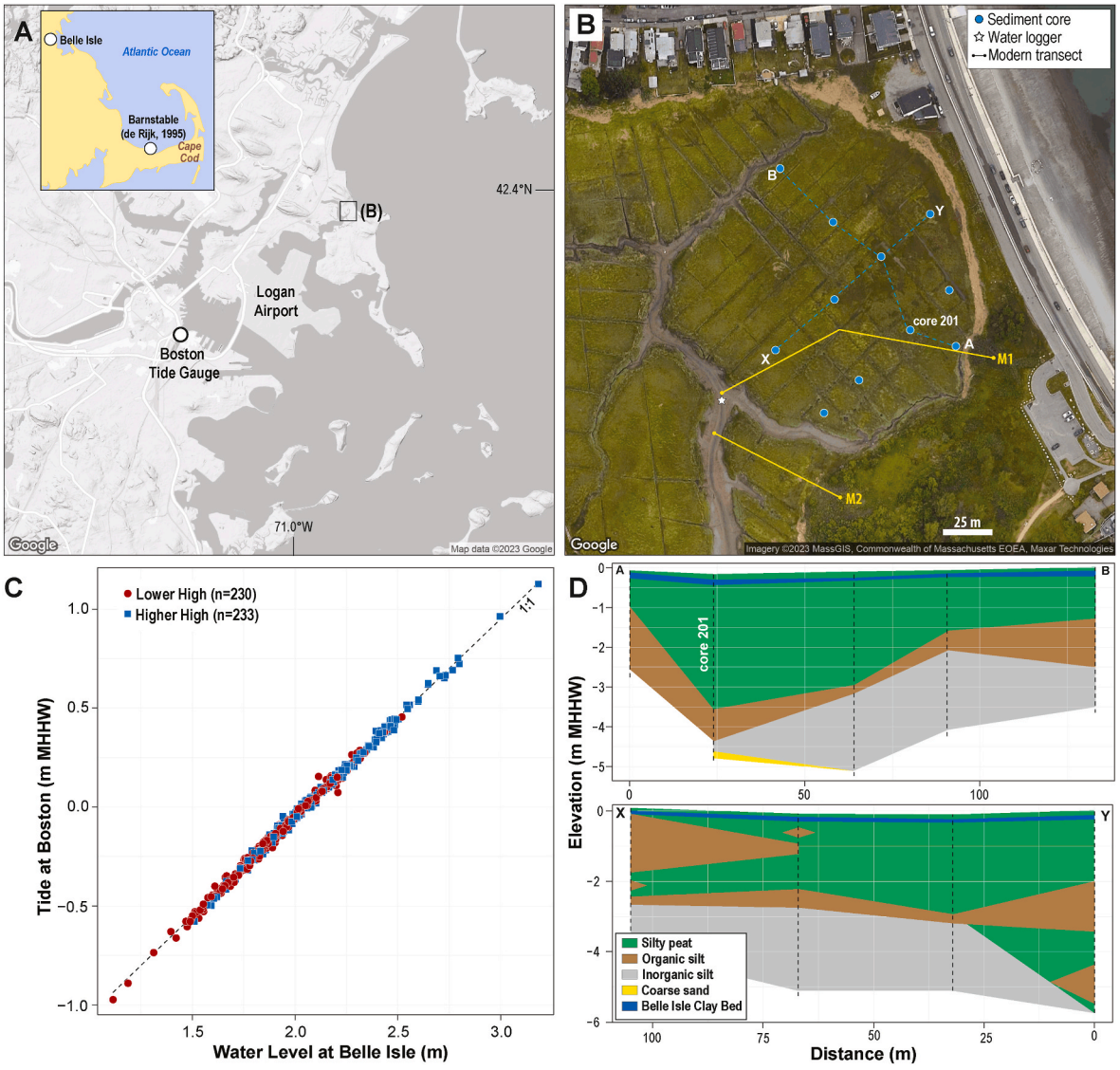

Fig. 1. **(A, B)** Location of study site at Belle Isle Marsh in Boston Harbor (base images are from Google Maps). Surface sediment samples were collected along modern transects M1 and M2. **(C)** Comparison of high tides (n = 463) measured at Belle Isle by an automated water-level logger (following correction for variability in atmospheric pressure) and by the Boston tide gauge. MHHW = mean higher high water. Coherence of tides between the locations demonstrates that the tidal prism defined for Boston is representative of tides at Belle Isle. **(D)** Stratigraphy beneath the Belle Isle salt-marsh described from hand-driven cores. Core 201 was selected for detailed analysis.

near-continuous RSL history to address the relative paucity of such data in the Gulf of Maine. In this capacity the new reconstruction offers insight into the patterns and causes of late Holocene RSL change in the western North Atlantic Ocean. Reconstructed RSL trends in Boston Harbor during the 19th and 20th centuries are contextualized with historic observations and investigations from documentary archives.

2. Study area

Salt marshes were widespread in Boston Harbor, but beginning in the late 18th century large areas were modified by filling to create new land above the level of high tide (Seasholes, 2018). The salt marsh at Belle Isle today (~1.4 km^2; Fig. 1) is the remaining (unfilled) tract of a larger system of marshes in east Boston that were filled, notably for the construction of Logan International Airport. The airport opened in 1923 CE on ~0.54 km^2 of filled land, but underwent its largest expansion between 1944 and 1946 CE when hydraulic dredging of sediment from the harbor bottom provided the fill material that was later topped with terrestrially-sourced sand and dirt; the airport now covers ~6.6 km^2 of made land (Seasholes, 2018).

The Belle Isle salt marsh is dissected by a large tidal creek (up to ~2 m deep), with an unvegetated, muddy bottom that is sub-aerially exposed at low tide and occupied by marine bivalves (especially mussels and snails). The vegetated salt marsh is comprised of a narrow band of *Spartina alterniflora* on creek banks levees that gives way to an expansive high-marsh platform vegetated by a mixed community of *Spartina patens* and *Distichlis spicata*. Small patches of stunted *Spartina alterniflora* are found in shallow, poorly-drained depressions within the high-marsh zone. The plants in these zones utilize the C_4 photosynthetic pathway, with the result that plant tissue yields $\delta^{13}C$ values of approximately −13‰, compared to approximately −32‰ to −21‰ in C_3 plant issue (Lamb et al., 2006). The transition from salt marsh to upland plant zones (and often urban development) is a narrow, brackish community dominated by reeds (*Phragmites australis*; C_3 plant) and shrubs (*Solidago sempervirens*, *Limonium nashi,* and *Suaeda linearis*; C_3 plants).

The Boston tide gauge (NOAA ID 8443970) is located ~6 km from Belle Isle (Fig. 1A). Annual RSL measurements are available since 1921 CE (Holgate et al., 2013) with 98% completeness. Piecuch et al. (2018) estimated that during the 20th century, RSL rose at 2.5 ± 0.8 mm/yr (95% credible interval), including a contribution of 0.9 ± 0.6 mm/yr from ongoing glacio-isostatic adjustment (GIA). This tide-gauge record was extended by Talke et al. (2018) using archival water-level and surveying measurements from the Charlestown Navy Yard to add 49 years of data between 1825 CE and 1911 CE. This archival research also brought to light earlier investigations, correspondence, and court cases with implications for how RSL change was observed and understood in late 19th and early 20th centuries.

3. Methods

3.1. Tidal elevations

An automated water-level logger was twice deployed (September 14, 2022 to November 28, 2022 CE and December 20, 2022 to June 6, 2023 CE) as low as possible in the tidal frame at Belle Isle to establish local tidal datums (Fig. 1B). Measurements were corrected for changes in local atmospheric pressure using a second logger placed above the limit of tidal inundation. High and low tides were then isolated using the VulnToolKit package for R (Hill and Anisfeld, 2021). Corresponding water-level measurements from the Boston tide gauge were processed in the same way. The strong correlation of tides between the two locations (Fig. 1C) confirms that measurements from the Boston tide gauge are appropriate for characterizing tides at Belle Isle. Subsequently, local tidal datums were established using NOAA definitions from measurements at the Boston tide gauge over a custom tidal epoch representing the ten years prior to sampling (2013–2022). The elevation of the water-level loggers was expressed relative to these tidal datums. Temporary benchmarks were established by leveling to the water loggers using a total station (Woodroffe and Barlow, 2015). All other leveling (e.g., core tops and surface samples) used the same total station and referenced measurements to the temporary benchmarks.

3.2. Stratigraphy and sampling

The stratigraphy beneath the Belle Isle salt marsh was described from hand-driven cores positioned along intersecting transects (Fig. 1B–D). Core 201 was recovered for further analysis using an Eijelkamp peat sampler to reduce contamination and sediment compaction. All core samples were transferred to split PVC tubes, wrapped in plastic, labeled, and stored in darkness at 4 °C for preservation. Core top elevations were measured using the method and instruments described in section 3.1.

3.3. History of sediment accumulation

Core 201 was dissected to isolate identifiable plant macrofossils with a known relationship to paleo salt-marsh surfaces. The macrofossils were predominantly the *in-situ* rhizomes and stems of common high salt-marsh plants (*Spartina patens* and *Distichlis spicata*) that grew at 2 ± 2 cm below the marsh surface, or material that was likely deposited on the marsh surface (e.g., seeds, fragments of wood). From this suite of material, samples were selected for radiocarbon dating to provide an approximately even distribution upcore.

All samples selected for radiocarbon dating were soaked in deionized and organic-free (MilliQ) water to remove salt and adhered sediment before being manually cleaned under a binocular microscope to remove any visible contaminating material, such as ingrowing younger rootlets (Kemp et al., 2013). The samples were then dried at ~40 °C and were either processed using standard acid-base-acid pretreatment, or no pretreatment. Five larger samples were divided into two pieces after cleaning to directly compare the effect of pretreatment.

All samples were submitted to the National Ocean Sciences Accelerator Mass Spectrometry (NOSAMS) laboratory where they underwent either traditional or single-step graphitization (Elder et al., 2019). Samples from this core were previously divided into two pieces to directly compare the effect of graphitization method (Sefton et al., 2022a, Fig. 2). This experiment demonstrated that single-step graphitization of plant macrofossils yielded radiocarbon ages that were as accurate as those from traditional graphitization, but with a modest increase in uncertainty (mean/maximum of 6.25/15 additional ^{14}C yrs). Following graphitization, radiocarbon was measured using standard AMS analysis. Six (none-replicated) samples were not converted to graphite, but rather radiocarbon was measured using a mini carbon dating system gas interface instrument (MICADAS; Synal et al., 2007) at NOSAMS.

Due to a plateau in the radiocarbon calibration curve, material less than ~300 years old can yield multiple intervals of calendar ages spanning a relative large period of time (Reimer et al., 2020). Consequently, estimates of sample age generated by age-depth models may be more uncertain than in older parts of the core. Recognition of pollution and land-use events of known age in upcore profiles of (for example) elemental abundance and isotopic activity (e.g., Marshall, 2015) reduces uncertainty in estimates of sample age by reducing the likelihood that some calibrated age ranges are compatible with stratigraphic ordering of samples. This effect can propagate to depths/ages below/older than the marker horizons (Sefton et al., 2022b).

Upcore Pb abundance and magnetic susceptibility were measured using the ITRAX x-ray fluorescence (with Bartington MS2E sensor) instrument at the University of Massachusetts Amherst. Due to natural heterogeneity of high salt-marsh sediment, measurements were averaged across 1-cm depth increments. Pb abundance is expressed as counts per second and magnetic susceptibility is expressed in standard international units (SI $\times 10^{-5}$). A consistent feature of the stratigraphy

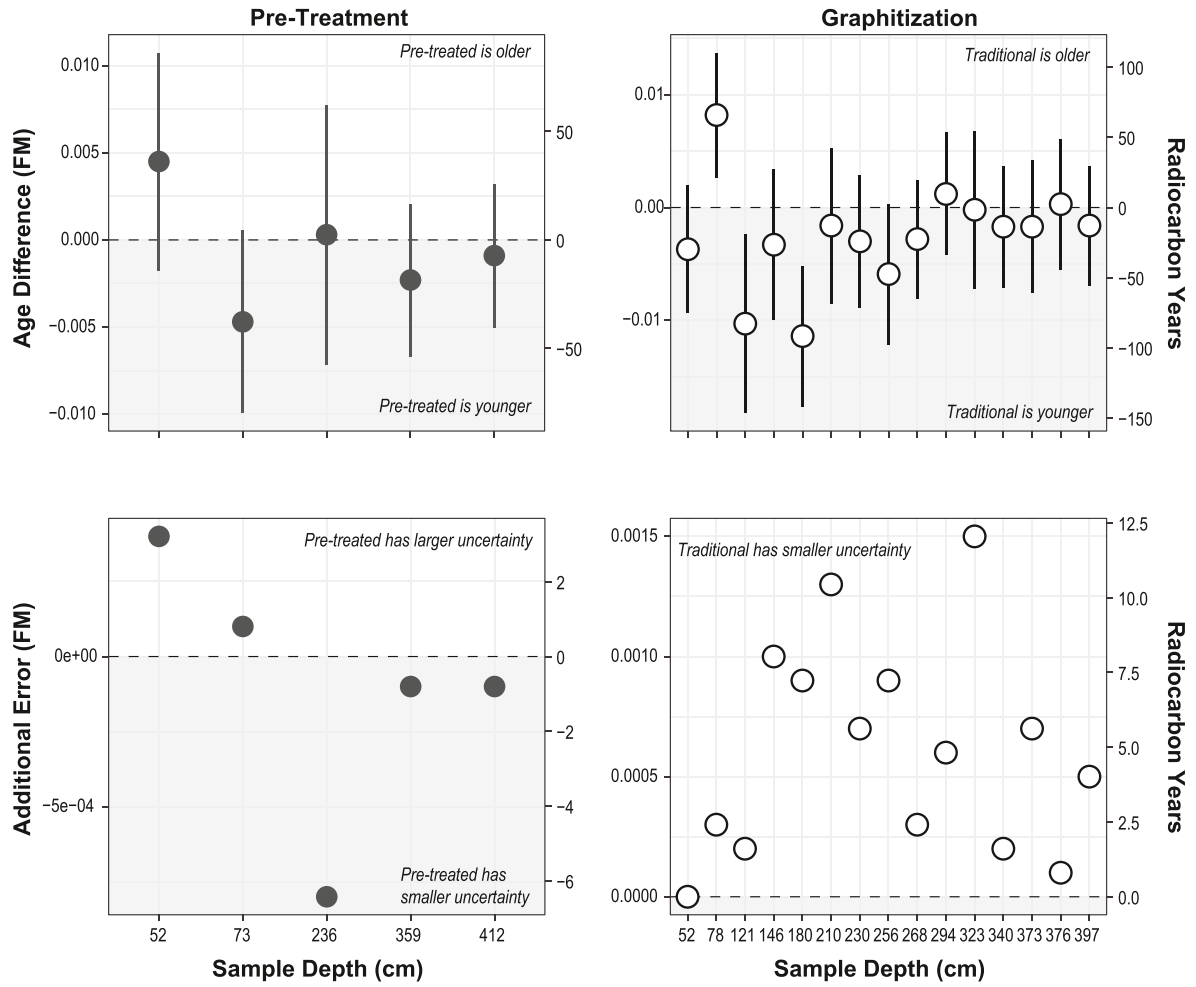

Fig. 2. Comparison of radiocarbon ages from replicate samples of common salt-marsh plant macrofossils (*Distichlis spicata* and *Spartina patens*). Left column is the effect of pretreatment (acid-base-acid or no pretreatment other than manual cleaning). Right column is the effect of graphitization method (traditional or single-step); data are reproduced from Sefton et al. (2022a). Top row of panels represents the difference in sample age between replicates. Error bars are the 95% confidence interval. Bottom row of panels represents the difference in reported uncertainty between replicates. Regions are shaded and labeled to show direction of difference among pretreatment and graphitization regimens. FM = fraction modern.

beneath the Belle Isle salt marsh is a shallow layer of blue-colored clay that we term the Belle Isle Clay Bed (Fig. 1D). The clay is likely Pleistocene-age Boston Blue Clay that was subsequently deposited in Boston Harbor and remobilized during the dredging that took place to expand Logan Airport in 1944–1946 CE (Seasholes, 2018). Some of the dredged material was carried to the nearby Belle Isle salt-marsh surface by tides, where it formed a distinctive stratigraphical horizon that contrasts with the underlying and overlying organic-rich salt-marsh sediment.

We produced an age-depth model for core 201 using the Bchron package for R (Parnell et al., 2008, 2011; Parnell and Gehrels, 2015). The position of radiocarbon-dated rhizomes was adjusted upward by 2 cm and assigned an uncertainty of ±2 cm since they grow within 4 cm of the salt-marsh surface (Supporting Table 1). The depth of samples interpreted as being deposited on a contemporary salt marsh surface were not adjusted. The Bchron age-depth model calibrated all radiocarbon ages using the IntCal20 calibration curve (Reimer et al., 2020). Horizons dated by recognition of pollution trends/events were treated as having normal-distributed uncertainty. We term the age-depth developed using all available dates the *master* chronology.

3.4. Simulating core chronologies

The high density of radiocarbon dates in core 201 facilitates simulation of plausible sampling decisions through repeated subsampling. We divided the core into seven depth intervals to balance the goals of having each interval be (approximately) the same thickness and include (approximately) the same number of radiocarbon dates. The thinnest/thickest intervals were 35/61 cm and each included 11–16 radiocarbon ages from either eight or nine unique depths (Fig. 3). In the simulated chronologies, radiocarbon dates were drawn randomly from each of the seven depth intervals with the criteria that a unique depth could not be sampled more than once in an iteration. A chronology was developed using only the sampled radiocarbon ages as input to Bchron and then a second time with all age markers added to the unchanged input of radiocarbon ages. This approach ensures fair comparison between chronologies with and without age-depth markers. This process was repeated 2000 times for sampling sizes of 1–8 radiocarbon ages in each of the seven depth intervals. The difference in sample age and uncertainty between each simulated chronology and the master chronology was calculated at all depths in the core.

3.5. Modern foraminifera and Bayesian transfer function

Fifty surface (0–1 cm) sediment samples were collected along two transects at Belle Isle (Fig. 1B) to characterize the modern relationship between foraminifera and tidal elevation. At the time of collection each sample was placed into a vial filled with buffered ethanol and Rose

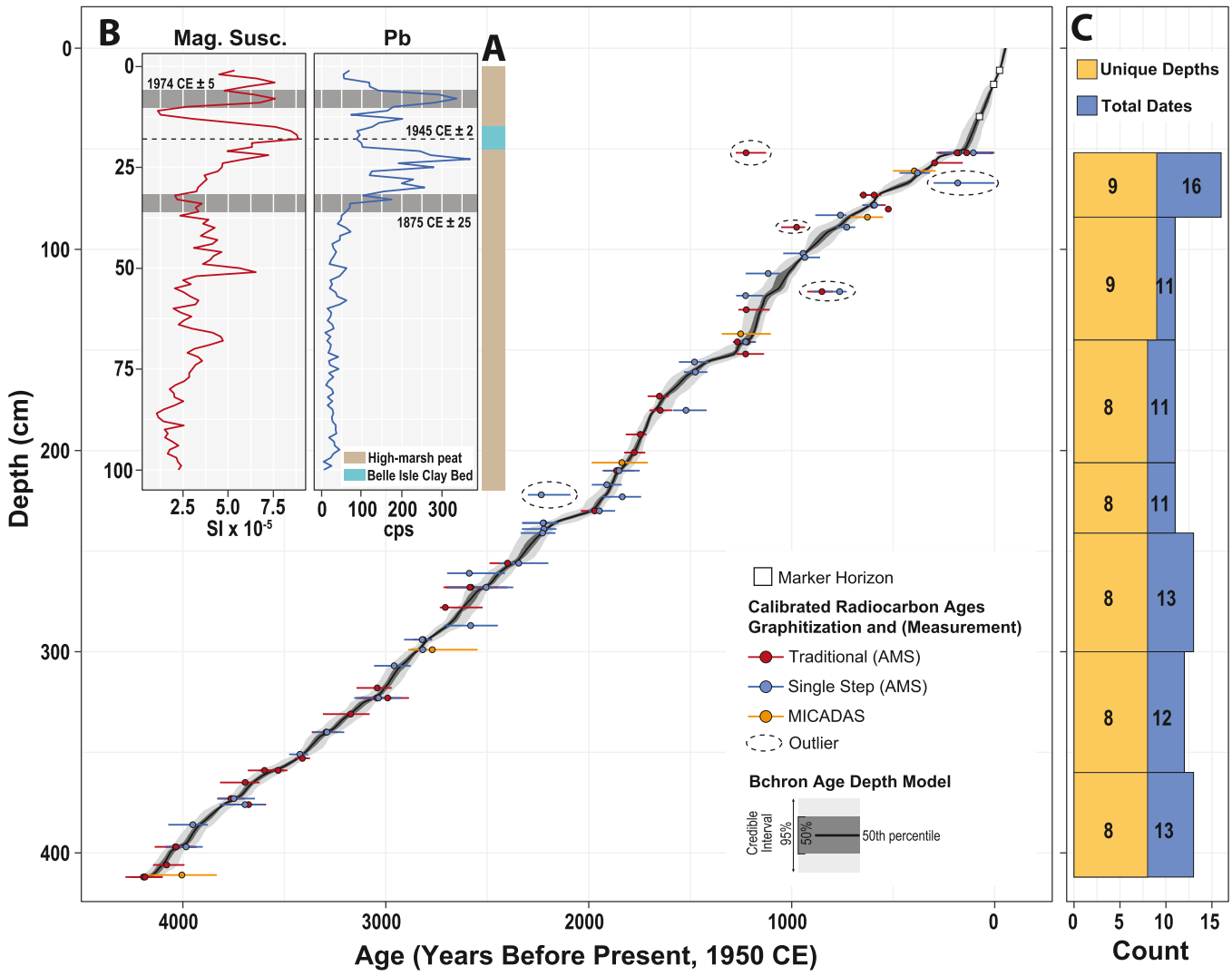

Fig. 3. Complete age-depth model for core 201 from Belle Isle. **(A)** Stratigraphic summary. The shallow Belle Isle Clay Bed is present throughout the site and interpreted as being deposited on the salt-marsh surface when nearby Logan Airport was expanded by dredging and filling in 1944–1946. **(B)** Age-depth model developed using all radiocarbon ages and marker horizons. This is termed the 'master' chronology in subsequent analysis. Calibrated radiocarbon dates show the modal age (symbol) and range (bars), but do not represent probability distributions within this range. Radiocarbon dates highlighted with dashed circles were part of the age-depth model input, which subsequently identified them as outliers. **(Inset)** Profiles of Pb concentration (expressed as counts per second, cps, integrated over 1-cm thick intervals) and magnetic susceptibility used to identify the onset and peak of industrial activity. Shaded horizons show the depth and age range used as input to the age-depth model. **(C)** Division of the core into intervals of approximately equal thickness and number of radiocarbon ages for resampling to simulate plausible sampling decisions. Some depths have more than one radiocarbon age because of data collected to examine replication between pretreatment regimens and graphitization methods.

Bengal stain to differentiate living and dead individuals (Walton, 1952). The vials were refrigerated in darkness prior to processing. Samples were sieved under running water to collect the 63–500 μm fraction, which was counted wet under a binocular microscope. Where possible, a minimum of 100 dead individuals were counted in each sample to quantify the assemblage (Kemp et al., 2020). Taxonomy followed Edwards and Wright (2015); we retain *Jadammina macrescens* (Filipescu and Kaminski, 2008) because of its ubiquitous use in the sea-level literature and this species is differentiated from *Balticammina pseudomacrescens* (Gehrels and van de Plassche, 1999).

de Rijk (1995a) documented modern salt-marsh foraminifera from Barnstable (~90 km south of Belle Isle; Fig. 1) using 189 samples collected in four parts of the Great Marshes. Four samples without elevations were removed prior to any further analysis. Sample elevations were reported relative to mean high water (MHW_{1992}) that was established using a month of water-logger measurements (see Table 1 of de Rijk and Troelstra, 1997). The specific month of water-level measurements varied among the four sampled areas. VDatum indicates that the tidal regime and range at Barnstable are the same as at Boston (Yang et al., 2013). Therefore, we used measurements from the Boston tide gauge to establish the elevations of MHW_{1992} relative to station datum. Subsequently, sample elevations from de Rijk (1995a) were converted to be relative to tidal datums defined using measurements from the Boston tide gauge for the ten-year period preceding sample collection (June 1983 to June 1992). This interval approximates the time represented by a 1-cm thick sample of surface sediment and mirrors the approach taken at Belle Isle. Taxon abundance is tabulated as percentages (dead assemblage) and test density in de Rijk (1995a,b); since it is unclear what volume of material was counted, we assumed that 100 dead tests were counted.

Surface samples of foraminifera from Belle Isle (this study) and Barnstable (de Rijk, 1995a) were combined to create a modern training set comprised 225 foraminifera-bearing (dead count ≥30) samples (Supporting Table 2). Since great diurnal tidal range at Belle Isle (3.13

m) and Barnstable (3.15 m) are near identical, sample elevations were not standardized using a water level index. This combined dataset was used to construct a Bayesian transfer function (BTF; Cahill et al., 2016) following screening to remove samples below mean tide level since the shelly, inorganic mud characterizing these environments is not analogous to sediment in the stratigraphy underlying the site. The highest occurrence of foraminifera was established using only the samples from Belle Isle; de Rijk (1995a) includes three samples with foraminifera above this elevation, which we removed from the training set because it is likely that count sizes were low. Therefore, the data used to generate the BTF comprised 212 samples. The BTF was implemented using the BTFr package for R and model performance was evaluated using 10-fold cross validation.

3.6. Stable isotopes in bulk sediment

Surface sediment from the Belle Isle modern transects and core (1-cm thick at 4-cm intervals) samples were freeze dried and milled to a fine, homogenized powder. Measurements of bulk-sediment $\delta^{13}C$ (relative to the Vienna Pee Dee Belemnite standard; ‰ VPDB) were made by the Yale University Analytical and Stable Isotope Center on a commercial basis. This analysis also produced measurements of total organic carbon (TOC), total nitrogen (from which the ratio of carbon to nitrogen (C:N) was calculated), and $\delta^{15}N$ (‰, relative to air).

Modern photosynthesizing plants draw CO_2 from an atmosphere that was enriched in ^{12}C through combustion of fossil fuels (the Suess effect; Keeling, 1979). This enrichment results in a systematic difference in the isotopic composition of modern and pre-industrial plants (and the bulk sediments to which they are a significant source of carbon). To improve the analogy between $\delta^{13}C$ values measured in modern and fossil samples (Wilson, 2017), we adjusted modern measurements by adding 2.0‰, which is the estimated Suess effect for the ten years prior to sample collection (Kwon et al., 2022). The Bchron age-depth model (section 3.3) estimated the age of each $\delta^{13}C$ sample in the core and we used this age to correct for the Suess effect using annual atmospheric values (Kwon et al., 2022). These adjusted measurements are referred to as $\delta^{13}C_{adj}$.

3.7. Reconstructing relative sea level

Foraminifera in the core were counted in alternating, 1-cm thick slices. Application of the BTF to these assemblages generated reconstructions of paleomarsh elevation (PME) with uncertainty. The BTF was applied twice, firstly without informative priors and secondly with informative priors established by comparison of upcore $\delta^{13}C$ measurements with those from the modern salt marsh at Belle Isle and sites with similar plant communities on the U.S. Atlantic coast (Kemp et al., 2012; Stearns et al., 2023; Walker et al., 2021). RSL was reconstructed by subtracting PME estimated by the BTF from measured sample elevation (depth in core below core top). Sample age was estimated from the master age-depth model.

The degree of analogy between assemblages of foraminifera in the modern training set and preserved in core 201 was quantified through four measures of dissimilarity (Bray, Chi-squared, Chord, and Euclidean) using the Analogue package in R (Simpson, 2007). The dissimilarity between all possible pairs of modern samples was calculated and the 20th percentile of this distribution was adopted as a threshold. If the dissimilarity between a core sample and its closest modern analog exceeded the threshold it was determined to lack a modern analogue. Samples lacking a modern analogue in at least two of the four metrics were excluded from the subsequent RSL reconstruction. In addition, samples with count sizes <30 were excluded.

3.8. Relative sea-level trends

Trends in RSL at Belle Isle were quantified by applying the Noisy Input Generalized Additive Model (NI-GAM) of Upton et al. (2024) using the reslr package. Model input was RSL reconstructed using informative priors; no tide-gauge data were included and no rate of GIA was applied. Simultaneously, this model decomposed RSL trends in the western North Atlantic Ocean through analysis of the 21 RSL reconstructions from Newfoundland to southern Florida described by Upton et al. (2024), with the addition of the new record from Belle Isle. Posterior predictions were made on a 50-year grid with 95% confidence intervals. Briefly, the decomposition employs a univariate spline to identify a non-linear signal common to all records, random slopes and intercepts to estimate the site-specific and temporally linear term, and a spatio-temporal spline to describe residual, non-linear, local variations.

4. Results

4.1. Influence of pre-treatment, graphitization, and measurement on radiocarbon ages

Five plant macrofossil samples (four *Distichlis spicata* and one *Spartina patens*) were each divided into two pieces to investigate the influence of pre-treatment on radiocarbon dating of common salt-marsh plant macrofossils (Fig. 2). For each replicated sample, the uncertainty of age difference between pre-treatment regimens includes zero. The minimum/maximum absolute difference was 0.0004 FM (fraction modern; 2.4 ^{14}C yrs/0.0047 FM; 37.8 ^{14}C yrs) with a mean of 0.00254 FM (20.4 ^{14}C yrs). Two replicates yielded an older age with acid-base-acid pretreatment, while three replicates yielded an older age without pretreatment. Differences in reported age uncertainty were small (three samples have a difference of less than one ^{14}C yr) and show no evidence of being systematic (when pretreated three have reduced uncertainty and two have increased uncertainty). In the context of rounding conventions for radiocarbon ages and their uncertainties (Stuiver and Polach, 1977), the differences among pre-treatment regimens for replicate samples are minimal.

In core 201, 41 macrofossils were processed using traditional graphitization prior to measurement by AMS and these samples yielded a mean uncertainty of 0.00184 FM (15 ^{14}C yrs), ranging from 0.0014 to 0.003 FM (11–24 ^{14}C yrs; Fig. 3). For comparison, the 40 samples that underwent single-step graphitization returned uncertainties with a mean of 0.00237 FM (19 ^{14}C yrs) and ranging from 0.0019 to 0.0033 FM (15–27 ^{14}C yrs). The small additional error associated with single-step graphitization ($\sim$4 ^{14}C yrs) is consistent with the results of Sefton et al. (2022b), who reported a mean difference of 6.25 ^{14}C yrs from replicated samples in this core (those results are included in this analysis; Fig. 2). Use of single-step graphitization to prepare salt-marsh plant macrofossils for radiocarbon dating does not result in a notable increase in uncertainty and there is no indication from these results (and the replicated samples analyzed by Sefton et al., 2022a) that there is a difference in accuracy.

Six (non-replicated and not pretreated) samples were not converted to graphite, but rather radiocarbon measurement was performed by feeding combustion gas into the MICADAS instrument at NOSAMS. The mean age uncertainty for these samples was 0.00612 FM (49 ^{14}C yrs) and ranged from 0.005 to 0.0072 FM (40–58 ^{14}C yrs). Therefore, the MICADAS system likely generates radiocarbon measurements for salt-marsh plant macrofossils with uncertainties that are three to four times larger than measurement by AMS (regardless of graphitization method).

4.2. Master age-depth model

The master age-depth model for core 201 was generated using Bchron (Parnell et al., 2008) with input from 87 radiocarbon dates (all pre-treatment, graphitization, and measurement types; provided as supplementary file) at 58 unique depths between 412 cm and 52 cm (Fig. 3). In addition, we identified three marker horizons that were used

in the age-depth model input. A pronounced increase in Pb concentration and magnetic susceptibility at 34 ± 2 cm was interpreted as the onset of industrialization and assigned an age of 1875 CE ± 25 years. At 20–15 cm the core stratigraphy is characterized by a layer of blue silt and clay with low organic content, that we termed the Belle Isle Clay Bed. It is likely material that was dredged from the harbor bottom in 1944–1946 CE to be used as fill material for expansion of Logan Airport (Seasholes, 2018). Notably, Pb concentration decreases sharply in this unit. While this change could be the result of a change in sediment type, it likely occurs because the dredged material was unpolluted having been deposited ~14,000 years ago (DeGroot et al., 2019). Magnetic susceptibility is relatively high because the clay bed is fine grained with low organic content. Decreasing Pb concentration in the uppermost ~11 cm of the core is likely caused by the passage of the Clean Air Act of 1970 and its subsequent success in decreasing atmospheric pollution. This horizon (at 13–9 cm) is assigned an age of 1974 ± 5 years.

Core 201 spans the past ~4200 years and the average age uncertainty (95% credible interval) for a 1-cm thick sample is ±52 years (range of ±13 to ±80 years; Fig. 3). Radiocarbon dates at five of the 58 unique depths are likely outliers (calibrated range does not overlap with the 95% credible interval of the age-depth model), including a replicate sample at 121 cm used to compare single-step and traditional graphitization (both replicates are outliers). Of the remaining outliers, two underwent traditional graphitization (both younger than expected) and two underwent single-step graphitization (one older and one younger than expected). This suggests that the selected plant macrofossils were outliers irrespective of the laboratory methods employed. These dates were part of the input to the age-depth model for constructing the master chronology. They were retained in the pool of dates available for selection during resampling because when isolated from the core and prepared for radiocarbon dating there was no indication that they would be unreliable.

4.3. Simulated chronologies

Plausible, alternative chronologies were generated for core 201 through repeated subsampling of the 87 available radiocarbon dates with the constraints that a unique depth could only be included once and each of the seven depth intervals must have the same number (1—8) of dates. This approach mirrors typical sampling efforts in studies aiming to build age-depth models for cores of salt-marsh sediment (and other Holocene sedimentary settings; e.g., Swindles et al., 2019). Each age-depth model estimated the age with uncertainty for every 1-cm increment of depth between 412 cm and the surface. The difference between these ages and those in the master chronology was calculated.

In simulated chronologies that excluded the three historic marker horizons of known age (at 34 cm, 18 cm, and 11 cm), depths above the uppermost radiocarbon date at 52 cm yielded large uncertainties (time spanned by the 95% credible interval). With one/eight radiocarbon date per depth interval, the average uncertainty was 461/230 years (compared to 112/83 years when the marker horizons were included). Below 52 cm the mean uncertainty in sample age decreases in an approximately exponential fashion as the number of radiocarbon dates in each depth interval increases (Fig. 4A). For example, with one radiocarbon date the mean uncertainty is 392 ± 37 (1σ) years for simulations that utilize only radiocarbon dates and 317 ± 34 years with the inclusion of marker horizons as input to the age-depth model. These uncertainties are 3.75 and 3.32 times larger respectively than those in the master chronology (Fig. 4B). With three radiocarbon dates the mean uncertainty is 211 ± 10/196 ± 20 years for chronologies without/with marker horizons, which corresponds to uncertainties that are approximately twice as large as those in the master chronology. With inclusion of five radiocarbon dates, parity (±1σ range that includes a value of 1; Fig. 4B) between the size of age uncertainties in the simulated and master chronologies is achieved for the first time. Inclusion of eight radiocarbon dates generates mean uncertainty of 127 ± 10 years with

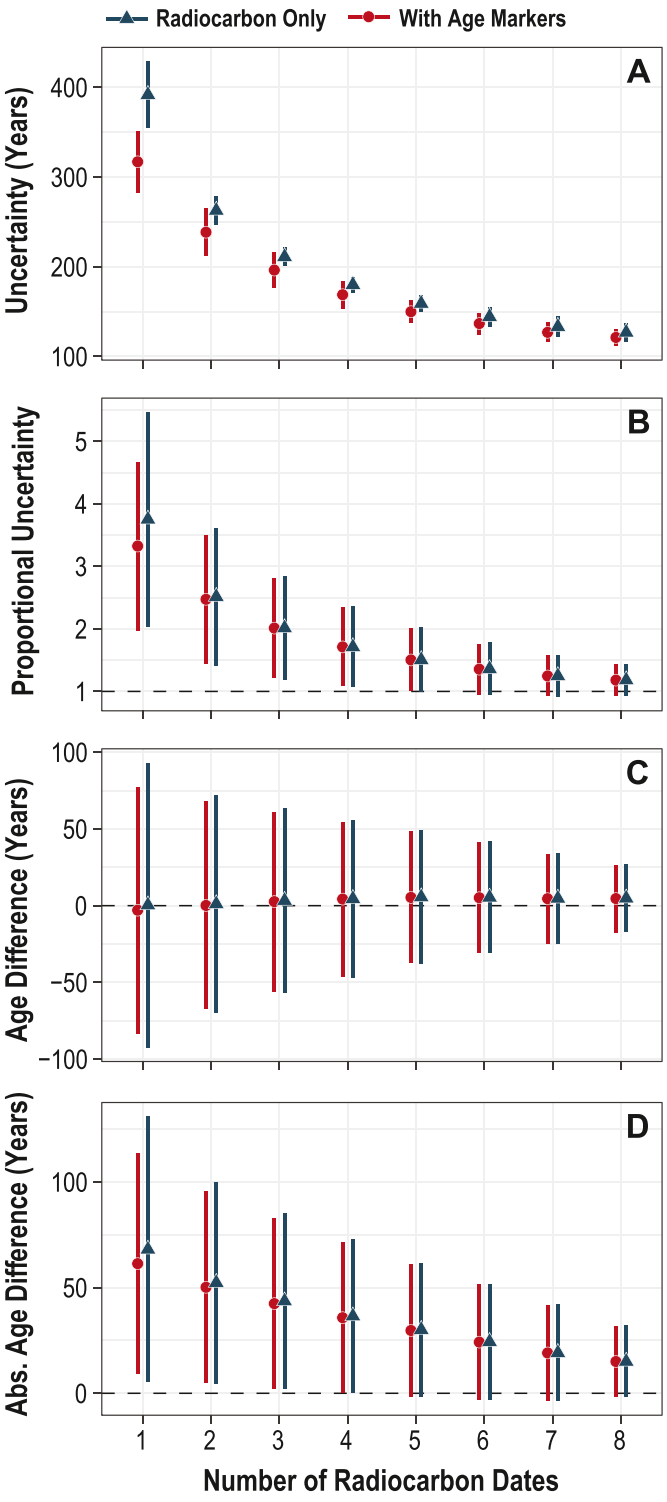

Fig. 4. Summary of plausible chronologies simulated by resampling of available radiocarbon dates. **(A)** Uncertainty for age-predicted by age-depth models. **(B)** Uncertainty for age in simulated chronologies expressed as a proportion of the uncertainty in the master chronology at the corresponding core depth. **(C)** Difference in age (50th percentile estimated by Bchron) between simulated chronologies and the master chronology. **(D)** As panel C, but absolute age difference. In each panel results are the mean (symbol) and standard deviation (bars) across all core depths and all iterations. Note that depths above 52 cm were excluded from analysis because the lack of radiocarbon dates as input results in anomalously large uncertainties at shallow depths for chronologies that used only radiocarbon dates. This facilities comparison with chronologies that utilized marker horizons (including the master).

only radiocarbon dates compared to 121 ± 9 years with markers, which is 1.2 times larger than the master chronology. These results suggest that chronologies using five radiocarbon dates per depth interval do not generate age-depth models that are markedly more uncertain than using eight or nine radiocarbon dates. The modest (but persistent) reduction in age uncertainty through inclusion of marker horizons indicates that they can increase precision even at lower depths in the core, particularly if there are relatively few radiocarbon dates.

Irrespective of the number of radiocarbon dates included in the simulated chronologies, the mean difference in sample age compared to the master chronology is less than six years (Fig. 4C), indicating that the difference is not systematic. However, the standard deviation of differences decreases sharply from 93/80 years without/with marker horizons when only one radiocarbon date per interval is included to 51/50 years with four radiocarbon dates and 22/22 years with eight radiocarbon dates (Fig. 4D).

In the master chronology there is qualitative evidence for two intervals (at 156—152 cm representing ~135 years and 236—230 cm representing ~180 years) of sedimentation occurring at markedly slower rates (~0.3 mm/yr) than the long-term rate (~1 mm/yr; Fig. 3). No change in stratigraphy was recognized in the field or lab at these core depths. The time represented by these two sections of the core was calculated (difference in mean age between the bounding depths) for each simulated chronology (Fig. 5). A relatively large difference in age

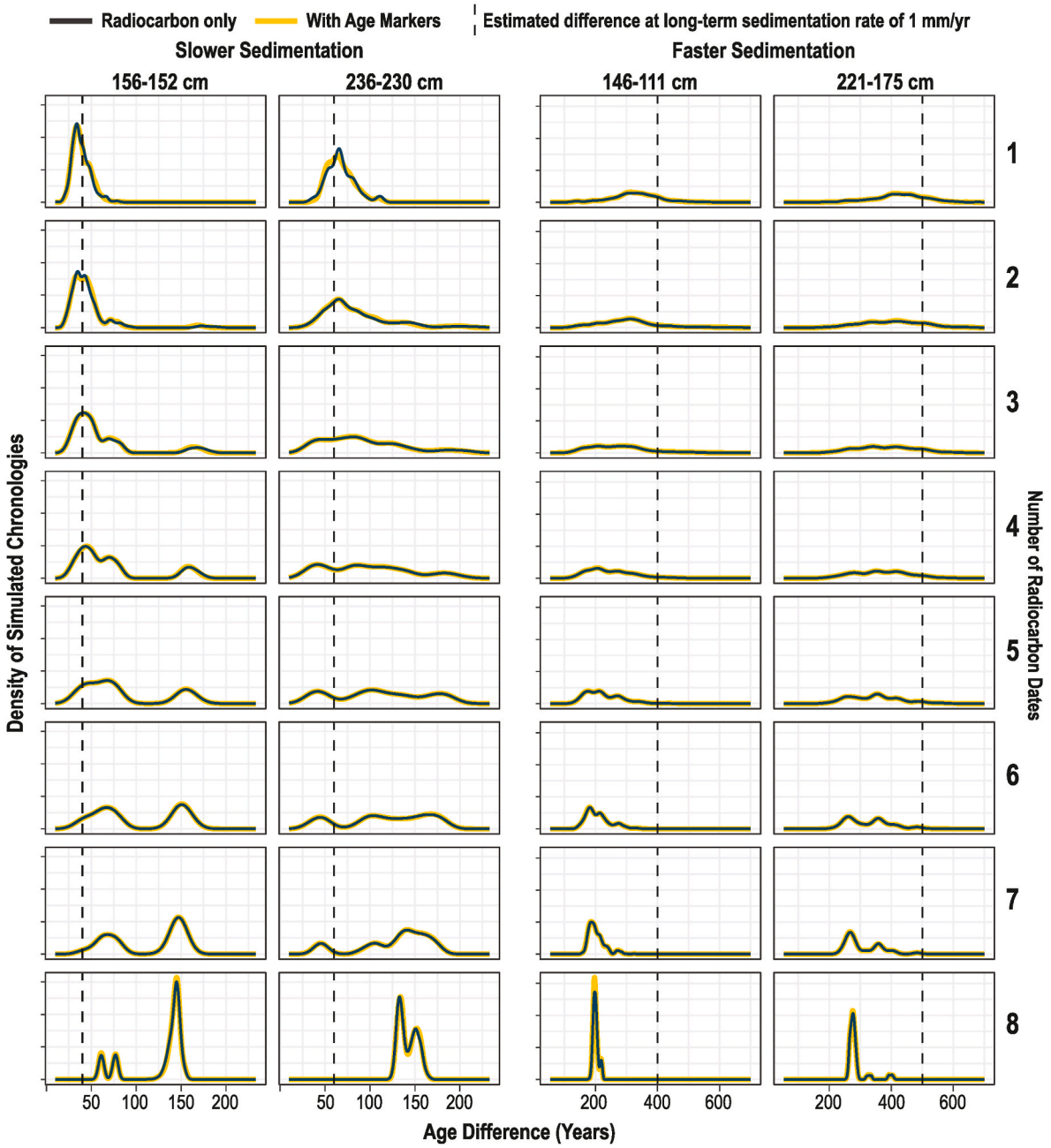

Fig. 5. Detection of intervals with sediment accumulation rates that depart from the long-term trend. Four periods (columns) were qualitatively interpreted as showing slower (156–152 cm and 236–230 cm) or faster (146–111 cm and 221–175 cm) sedimentation. In each simulated chronology with varying number of radiocarbon dates in core sections of approximately equal thickness (rows), the time represented by these intervals (duration) was calculated as the difference between mean age at the upper and lower depths. The duration corresponding to a long-term sedimentation rate of 1 mm/yr is represented by a reference line. Shorter/longer durations than this reference convey faster/slower sedimentation rates.

would indicate that slower sedimentation could be identified, while a difference in age close to the long-term sedimentation rate would suggest that the change in sedimentation rate is unlikely to be recognized. In all instances, the likelihood of identifying slower sedimentation is consistent for chronologies generated with and without historic markers. For the possible slower sedimentation at 156–152 cm, simulated chronologies with two radiocarbon dates in each depth interval suggest that this section of core most likely represents ~40 years, which is consistent with long-term sedimentation at ~1 mm/yr (i.e., the slower sedimentation is not detected). As the number of radiocarbon dates increases the estimated time span increases, but there is pronounced uncertainty in just how long is represented until eight radiocarbon dates are included and the most likely duration is ~140 years (equating to ~0.3 mm/yr; Fig. 5). A similar pattern is observed for the possible slower sedimentation at 236–230 cm. With two radiocarbon dates per interval the most likely time span is ~60 years, which lies close to the long-term sedimentation rate. Only when the density of radiocarbon dates is increased to eight per interval does slower sedimentation emerge (lasting ~130 years).

Periods of sedimentation qualitatively faster than the long-term rate of ~1 mm/yr occur in the master chronology at 146–111 cm (spanning ~225 years at ~1.6 mm/yr) and 221–175 cm (spanning ~270 years at

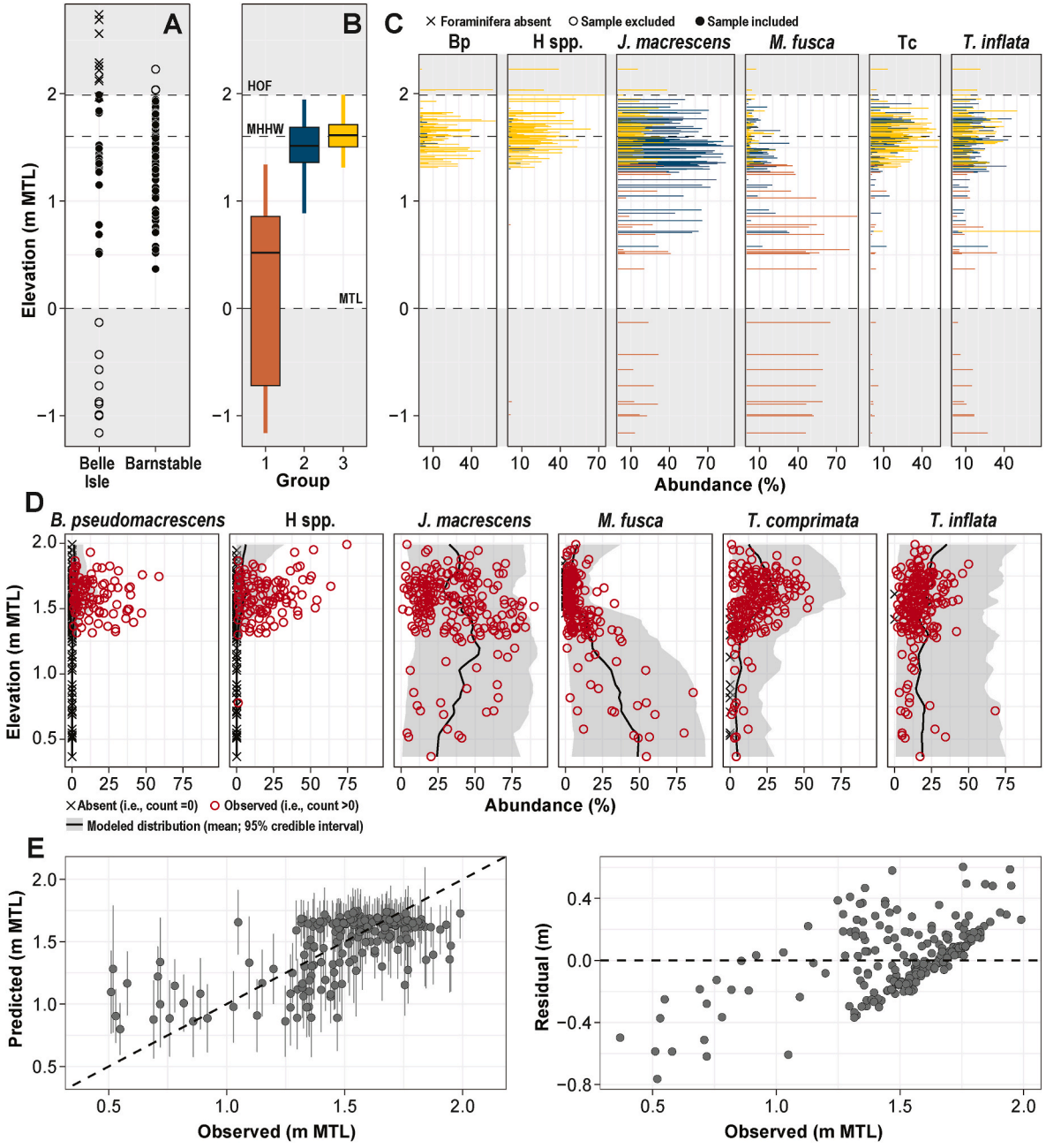

Fig. 6. Relationship between foraminifera and elevation at Belle Isle (this study) and Barnstable (de Rijk, 1995a). **(A)** Distribution of samples by elevation. MTL = mean tide level. **(B)** Elevation of foraminiferal assemblages identified by partitioning around medoids. Boxes represent the 25th, 50th, and 75th percentiles. Whiskers extend to the largest value no further than 1.5 times the interquartile range from the hinge. MHHW = mean higher high water, HOF = highest occurrence of foraminifera. **(C)** Relative abundance of surface foraminifera. Sample shading denotes group membership. Bp = *Balticammina pseudomacrescens*, H spp. = *Haplophragmoides* spp., Tc = *Tiphotrocha comprimata*. **(D)** Relationship between the principal taxa of foraminifera and elevation defined by species response curves from the Bayesian transfer function. Symbols differentiate whether each taxon was present (count>0) or absent (count = 0) in each sample. **(E)** Cross-validated (10-fold) performance of a Bayesian transfer function for reconstructing paleomarsh elevation using assemblages of foraminifera.

~1.7 mm/yr; Fig. 3). We evaluated how readily these intervals might be detected in age-depth models using the same approach adopted for slower sedimentation (Fig. 5). A smaller difference in age through the depth intervals would indicate faster sedimentation, while a larger difference would suggest accumulation of sediment at a rate closer to the long-term trend. Even with a single radiocarbon depth in each section of the core the modal density indicates that sedimentation likely exceeded the background trend for both examples. With additional radiocarbon dates it becomes increasingly likely that a period of faster sedimentation could be identified and with five or more dates there is a low likelihood that either interval is characterized by background rates of accumulation.

4.4. Modern distribution of sea-level proxies

The modern training set of salt-marsh foraminifera from Belle Isle and Barnstable (de Rijk, 1995a) is comprised 225 samples with at least 30 dead tests and measurements of tidal elevation. These samples are distributed from −1.16 m to 2.23 m MTL. (Fig. 6A). At Belle Isle the highest occurrence of foraminifera is at 1.99 m MTL. This threshold is used for the combined dataset because it is unclear how many tests were present in the higher assemblages described at Barnstable. Cluster analysis (Partitioning Around Medoids; Rousseeuw, 1987) identified three groups of foraminifera (Fig. 6B). Group 1 includes 25 samples with relatively high abundance of *Miliammina fusca* (mean 52%; Fig. 6C). This group was present at both sites and occurs from −1.16 m MTL (lowest sample in dataset) to 1.34 m MTL with a mean/median elevation of 0.21/0.52 m MTL. It is associated with tidal flats, and the lower, seaward edge of the salt-marsh platform. Group 2 represents 96 samples in which *Jadammina macrescens* (mean 55%) and *Trochammina inflata* (mean 17%) are the most common taxa. This group was present at both sites above 0.58 m MTL with a mean/median elevation of 1.49/1.52 m MTL. It is associated with high salt-marsh environments and the transition into a brackish plant community above MHHW. Group 3 is comprised 104 samples with a more diverse assemblage than group 2 of *Tiphotrocha comprimata* (mean 32%), *Haplophragmoides* spp. (mean 20%), *J. macrescens* (mean 17%), *T. inflata* (mean 16%), and *Balticammina pesudomacrescens* (mean 13%). This group was present at both sites above 0.72 m MTL with a mean/median elevation of 1.62/1.61 m MTL. A BTF was generated using 212 samples at Belle Isle and Barnstable collected between MTL and the highest occurrence of foraminifera. Under cross validation, measured sample elevation lies within the 68/95% credible interval for predicted elevation for 142/201 of the samples (Fig. 6E). Cross validated residuals (difference between observed and predicted elevation), display some structure where samples from low/high elevations are over/under predicted.

The stable isotopic composition of bulk salt-marsh sediment was measured on the 50 surface samples from Belle Isle (Fig. 7). Ten samples of tidal-flat mud located below MTL yielded a mean $\delta^{13}C_{adj}$ of −15.0‰. Five samples collected on creek bank levees (0.53–1.15 m MTL) vegetated by *Spartina alterniflora* are characterized by a mean $\delta^{13}C_{adj}$ of −16.1‰. On the salt-marsh platform (1.27–1.52 m MTL), 21 samples dominated by *Spartina patens* and *Distichlis spicata* with occasional stunted *Spartina alterniflora* yielded a mean $\delta^{13}C_{adj}$ of −15.4‰. In the community of brackish vegetation, 14 samples (1.82–2.74 m MTL) collected above MHHW (1.56 m MTL) are characterized by a mean $\delta^{13}C_{adj}$ of −24.5‰. Nine of these 14 samples contained fewer than 30 dead foraminifera and were determined to lie above the highest occurrence of foraminifera (1.99 m MTL). The data from Belle Isle were combined with similar datasets from Rhode Island (Stearns et al., 2023), northern New Jersey (Walker et al., 2021), southern New Jersey (Kemp et al., 2012), and Delaware (Horton, unpublished). For each dataset, tidal elevation was calculated from the preceding ten years of water-level measurements at a nearby tide gauge and the same interval was the basis for correcting for the Suess effect. In the combined dataset there are 120 samples with $\delta^{13}C_{adj}$ values less negative than −17‰, of which 111 (93%) accumulated below MHHW. The samples in this group collected above MHHW are predominantly from northern New Jersey. A total of 71 samples are more negative than −20‰, of which 52 (73%) accumulated above MHHW. The 19 samples in this group collected below MHHW include 11 from Delaware.

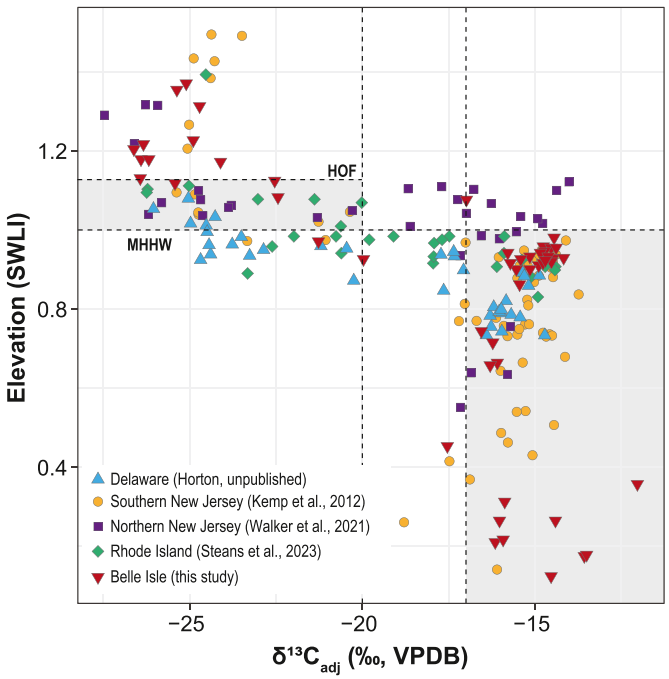

Fig. 7. Compilation of bulk-sediment $\delta^{13}C$ values from salt marshes in the northeastern United States. Elevation is expressed as a standardized water level index (SWLI; where 1 corresponds to mean higher high water, MHHW, and 0 to mean lower low water) to account for differences in tidal range among sites and was calculated from water-level measurements at nearby tide gauges for the ten years preceding sample collection. HOF is the highest occurrence of foraminifera at Belle Isle. Measured $\delta^{13}C$ values were corrected for the Suess effect using observations (Kwon et al., 2022) from the ten years preceding sample collection. Sample shape and shading denotes region where samples were collected. Dashed lines show chosen threshold elevation and $\delta^{13}C_{adj}$ values.

4.5. Sea-level proxies in core 201

Approximately 23,000 foraminifera were counted at 210 depths in core 201 between 412 cm and the surface (Fig. 8; Supporting Table 3). Five samples yielded fewer than 30 tests, while samples with 30–99 tests were disproportionately situated at 166-94 cm. Fifteen samples lacked modern analogs (Fig. 8) because they included unusually high abundances of *Miliammina petila* (20–48%, compared to a mean of <2% at all other depths; this species was not identified in the modern training set).

Between 412 cm and 26 cm, the mean, cumulative abundance of *Jadammina macrescens*, *Trochammina inflata*, and *Tiphotrocha comprimata* was 88.5%, while *Miliammina fusca* comprised 0.3% of tests. From 24 cm upward the occurrence of *Miliammina fusca* increased to a mean of 33.4%. This trend suggests that a relatively stable high salt-marsh environment persisted from 2163 BCE (mean age at 408 cm in the master chronology; Fig. 3) until 1913 CE (mean age at 26 cm in the master chronology), when the surface likely decreased in elevation relative to tidal datums. This inference is quantified by application of the BTF without priors, which shows that the high salt-marsh assemblages accumulated at an elevation close to MHHW (mean of 1.59 m MTL; Fig. 8) and yielded a mean uncertainty of 0.32 m (equating to ~10% of great diurnal tidal range), while the mean PME of the 13 samples with high abundances of *Miliammina fusca* was 0.98 m MTL with a mean uncertainty of 0.31 m. Notably, the rise in *Miliammina fusca* is

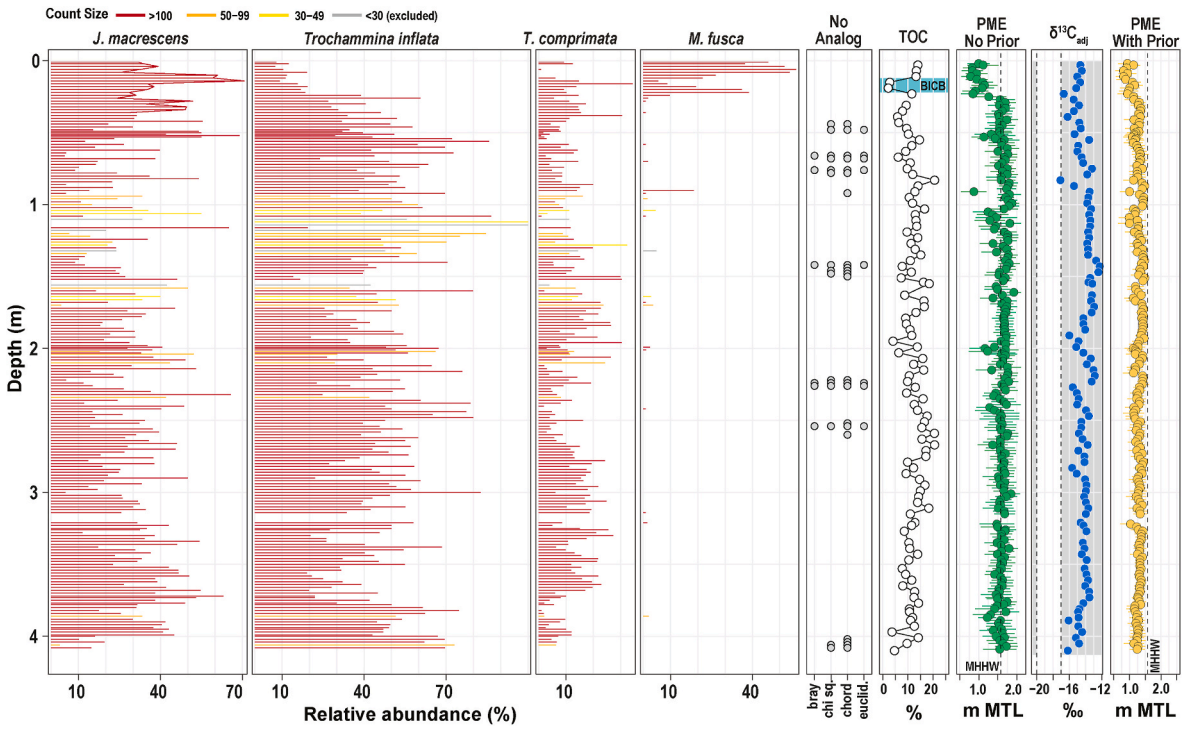

Fig. 8. Sea-level proxies preserved in core 201 and reconstructions of paleomarsh elevation (PME). Foraminifera are presented as percentage data with bar color showing the number of individual tests counted. The dissimilarity between modern and fossil foraminiferal assemblages was measured using four distance metrics. If the dissimilarity between a fossil sample and its closest modern analog exceeded the 20th percentile of dissimilarity among all possible pairs of modern samples it was deemed to have no modern analog. For clarity of presentation only samples and metrics returning no modern analog outcomes are shown; all other samples and metrics indicated a modern analog. TOC = Total Organic Carbon; BICB = Belle Isle Clay Bed. A Bayesian transfer function was applied to the foraminiferal assemblages to reconstruct PME (relative to mean tide level, MTL) without informative priors and then with priors informed by bulk-sediment $\delta^{13}C_{adj}$ values to identify sediment that likely accumulated above (more depleted than −20‰, dashed vertical line) or below (less depleted than −17‰, dashed vertical line) the mean higher high water (MHHW) tidal datum.

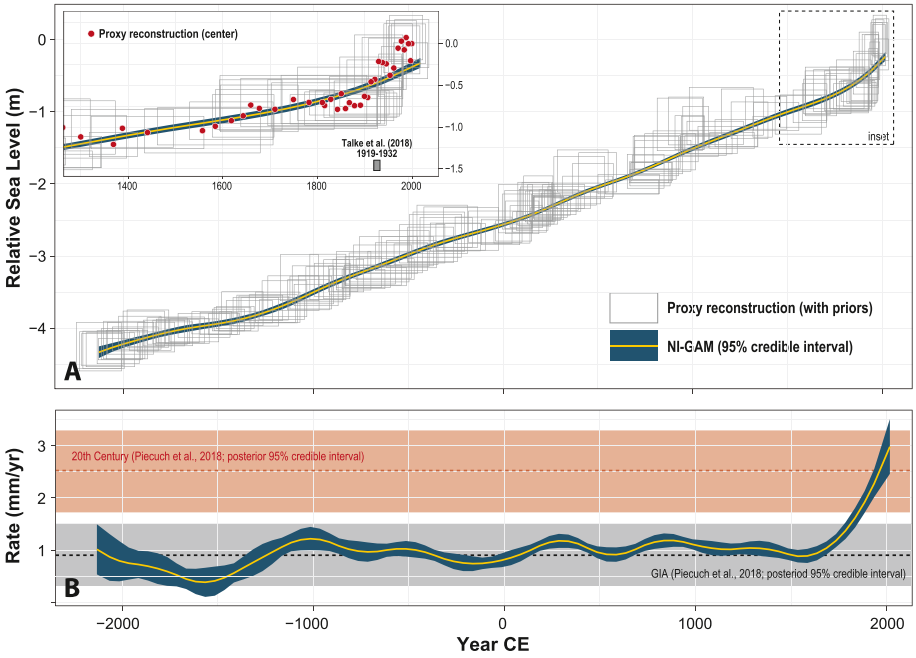

Fig. 9. **(A)** Relative sea-level reconstruction from Belle Isle in Boston Harbor. The presented reconstruction used informative priors from bulk-sediment $\delta^{13}C$ when the Bayesian transfer function was applied to fossil assemblages of foraminifera. The proxy reconstruction is represented by boxes that capture the 95% confidence interval for sample age and elevation, the center point of reconstructions are presented only in the inset panel. The noisy input generalized additive model (NI-GAM) did not incorporate tide-gauge data. **(B)** Rate of relative sea-level change estimated by the NI-GAM, compared to estimated rates of change for Boston during the 20th century and caused by glacio-isostatic adjustment (GIA) from Piecuch et al. (2018).

punctuated by a reduced relative abundance in the ~8-cm thick Belle Isle Clay Bed that was deposited rapidly at the time of Logan Airport's construction (Fig. 8). This trend is ecologically plausible since the deposited material would have briefly elevated the salt-marsh surface relative to local tides.

Bulk sediment $\delta^{13}C$ values measured in 101 bulk sediment samples were less negative than −17‰ (following correction for the Suess effect when necessary), while one sample was more negative (−17.1‰; Fig. 8; Supporting Table 3). Therefore, all depths in the core were assigned an informative prior of having formed below MHHW because they were likely vegetated by C_4 plants. Application of the BTF with priors accordingly lowered the reconstructed PME for samples dominated by high salt-marsh taxa to 1.29 m MTL with a decrease of mean uncertainty to 0.21 m (equating to ~7% of great diurnal tidal range). In contrast, PME reconstructed for the samples with high abundances of *Miliammina fusca* was largely unchanged by adopting priors (mean PME 0.98 m and uncertainty of 0.27 m). The inferred loss of marsh elevation since the early 20th century is reduced from ~0.6 m without priors to ~0.3 m with informative priors.

4.6. Late Holocene relative sea-level change at Belle Isle

The RSL reconstruction from Belle Isle is comprised 190 data points with a mean vertical uncertainty of ±0.21 m and mean age uncertainty of ±105 years that are described using the NI-GAM (Fig. 9A; Supporting Table 3). Since 2130 BCE, RSL rose by 4.33 m. Prior to 1900 CE, the mean rate of RSL rise was 0.95 mm/yr (Fig. 9B), which is similar to the estimated contribution from GIA during the 20th century of 0.90 mm/yr (0.32–1.5 mm/yr 95% credible interval; Piecuch et al., 2018). The first time that the estimated rate of RSL rise at Belle Isle exceeded the contribution from GIA was likely between 1835 CE (mean rate >1.5 mm/yr) and 1885 CE (lower rate of the 95% credible interval >1.5 mm/yr). Since 1900 CE, the salt-marsh reconstruction captures ~0.29 m of RSL rise at an accelerating rate, which reached 2.98 mm/yr (2.46–3.51 mm/yr 95% credible interval) in 2017 CE. For comparison, Piecuch et al. (2018) estimated the rate of RSL at Boston since 1900 CE to be 2.52 mm/yr (1.72–3.27 mm/yr 95% credible interval) and NOAA report the linear RSL trend at Boston to be 2.94 mm/yr for 1921–2023 CE.

5. Discussion

5.1. Chronologies of salt-marsh sediment accumulation

5.1.1. Preparation, graphitization, and measurement of radiocarbon in salt-marsh macrofossils

Efforts to generate near-continuous, late Holocene RSL reconstructions rely on using age-depth models to quantify the history of sediment accumulation in salt marshes. For material younger than ~200 years old there are several possible dating methods that can be employed such as ^{210}Pb and recognition of local- (e.g., the Belle Isle Clay Bed deposited in Boston Harbor during airport expansion), regional- (e.g., metals pollution from industrialization in the northeastern United States and Canadian Maritimes; Dunnington et al., 2020; Lima et al., 2005), and global-scale (e.g., ^{137}Cs and plutonium isotopes; Corbett and Walsh, 2015; Waters and Turner, 2022) marker horizons of known age in stratigraphic, elemental, isotopic, and pollen profiles. However, for sediment older than ~200 years, radiocarbon dating is often the only viable method for direct dating. On the Atlantic coast of North America, salt-marsh sediment preserves rhizomes and stems that can often be identified to the species level (Niering et al., 1977) and these woody plant macrofossils are the preferred sample material for radiocarbon dating (van de Plassche, 1991; Wright et al., 2017). Such samples are typically cleaned before submission (Kemp et al., 2013) to a radiocarbon dating lab where they undergo acid-base-acid pretreatment (e.g., Brock et al., 2010), followed by graphitization, and measurement by AMS.

Replicate samples from Belle Isle (Fig. 2) indicate that there is no systematic or pronounced difference in sample age (and uncertainty) between manually-cleaned salt-marsh plant macrofossils that underwent no pretreatment and those that were processed using acid-base-acid pretreatment following manual cleaning. This is likely because the woody nature of rhizomes and stems of salt-marsh plants minimizes contamination by carbonates or organic acids. Therefore, it may be possible to reduce the time and financial burden of radiocarbon dating salt-marsh plant macrofossils (at least examples of *Spartina patens* and *Distichlis spicata*) by employing a pre-treatment regimen that focuses on manual cleaning rather than chemical washes. This may be particularly advantageous for fragile samples that can experience considerable mass loss during chemical pretreatment (Norris et al., 2020). Furthermore, differences in pretreatment methods among studies are unlikely to be the cause for differences in RSL reconstructions and there is no suggestion that choice of pre-treatment regimen would bias resulting RSL records.

Previously a set of samples from core 201 were prepared in duplicate to compare the influence of graphitization method on AMS radiocarbon ages (Sefton et al., 2022a, Fig. 2). There was no discernible difference in sample age between methods and single-step graphitization delivered only a modest increase in reported radiocarbon uncertainty (mean 6.25 ^{14}C yrs), but with a ~50% cost reduction compared to traditional graphitization. Although the additional radiocarbon dates generated for this study do not include new replicates, the consistency of sample type (macrofossils of *Spartina patens* and *Distichlis spicata*) suggests that choice of graphitization method does not bias radiocarbon ages or their uncertainty. Therefore, the conclusion of Sefton et al. (2022a) that dating twice as many depths using single-step graphitization provides a cost-neutral means to increase the precision of age-depth models compared to relying exclusively on traditional graphitization is robust.

5.1.2. Influence of radiocarbon date density on sedimentation chronologies in salt marshes

A goal in reconstructing late Holocene RSL from single cores of salt-marsh sediment is to generate a near-continuous history with the potential to identify periods of relatively short-lived (century-scale) variability. The (in)ability to detect such changes in sequences of high salt-marsh sediment rests on how well the underlying age-depth model captures intervals of slower or faster accumulation. The time represented by two possible intervals of slower sedimentation in core 201 increased as more radiocarbon dates were included in the simulated chronologies (Fig. 5). With three or fewer radiocarbon dates per core section (corresponding to one date every ~15 cm), slower sedimentation is unlikely to be detected as evidenced by most age-depth models estimating no deviations from the long-term accumulation rate. With seven or more radiocarbon dates in each core section (corresponding to one date every ~5 cm) slower sedimentation became a feature in most of the simulated chronologies. Intervals characterized by faster sedimentation rates are more easily detectable. Even with one radiocarbon date in each core section the modal rate of sedimentation exceeds background rates and with three of more dates most simulated chronologies capture the deviation (Fig. 5). In 11 near-continuous RSL reconstructions produced from salt-marsh sediment between North Carolina and Newfoundland, the average density of radiocarbon dates was one date every 9 cm (ranging among cores from 14 cm to 4 cm). This suggests that existing late Holocene RSL reconstructions have an adequate density of radiocarbon ages to identify faster periods of accumulation, but that slower sedimentation (or more specifically periods where physical processes cause reduced rates of RSL rise) could be overlooked in some instances. Adopting single-step graphitization for preparation of plant macrofossils for radiocarbon dating presents an opportunity to increase the density of dates and increase the likelihood of detecting intervals of markedly slower accumulation (Sefton et al., 2022a). Inclusion of marker horizons does not influence detection of slower or faster sedimentation in deeper, pre-anthropogenic core

material.

5.2. Sea-level proxies in Boston Harbor

5.2.1. Foraminifera

Foraminifera are the most-commonly employed proxy in studies seeking to reconstruct RSL from salt-marsh sediment because they form low-diversity assemblages that occupy characteristic tidal elevations and are well preserved (Gehrels et al., 2020; Horton and Edwards, 2006). Using foraminifera to reconstruct RSL (or more specifically paleomarsh elevation) requires a training set that quantifies the observable relationship between modern foraminifera and elevation in environments analogous to those likely to be encountered in core material. Although the Atlantic coast of North America has a high density of modern datasets, there is a relative scarcity of such information from the study area. Extensive datasets exist for southern New England (Stearns et al., 2023; compiled from several earlier studies), Maine (Gehrels, 2000), and Nova Scotia (Scott and Medioli, 1980). Notably, these studies from neighboring regions (and many others from farther afield) concluded that salt-marsh foraminifera demonstrated a strong relationship to tidal elevation and are therefore sea-level proxies. In contrast, the modern data from Barnstable (Fig. 1), was previously interpreted as evidence that foraminifera represented salinity rather than elevation (de Rijk, 1995a, 1995b; de Rijk and Troelstra, 1997), suggesting that they have limited utility as sea-level proxies. The expanded modern dataset suggests that assemblages of foraminifera have a relationship to tidal elevation in Massachusetts (Fig. 6). Lower elevations are occupied by an assemblage with abundant *Miliammina fusca*, while two different assemblages are present in high salt-marsh environments above ~1 m MTL. We propose that the poor vertical zonation described previously at Barnstable reflects a paucity of samples collected below ~1 m MTL, with the effect that differences among neighboring high salt-marsh zones are evident, but differences among adjacent low and high salt-marsh zones are overlooked. The expanded modern training set displays vertical zonation of salt-marsh foraminifera and indicates that foraminifera can be employed as sea-level proxies as they are in other regions along the Atlantic coast of North America (Edwards et al., 2004; Gehrels, 2000) and beyond (Hawkes et al., 2010; Williams et al., 2021).

5.2.2. Bulk-sediment $\delta^{13}C$ values

Salt marshes in the U.S. mid-Atlantic and New England regions are unusual because they are often (and natively) dominated by the C_4 plants *Spartina alterniflora*, *Spartina patens*, and *Distichlis spicata* (Eleuterius, 1976; Niering et al., 1977; Redfield, 1972). These plants fractionate less strongly against molecules of $^{13}CO_2$ during photosynthesis than C_3 plants, with the result that their tissue yields less negative $\delta^{13}C$ values than C_3 plants (Chmura and Aharon, 1995; Lamb et al., 2006). The use of bulk-sediment $\delta^{13}C$ values as a sea-level proxy is premised on three assumptions: (1) C_4 communities have a systematic relationship to tides; (2) the organic carbon accumulating on the surface of a salt marsh is principally sourced from the in-situ plant community; and (3) surface sediment is incorporated into the stratigraphic record without sufficient post-depositional alteration or contamination of $\delta^{13}C$ values to inhibit recognition of botanical communities (Wilson et al., 2024).

Salt-marsh plants form distinctive zones where the boundaries between adjacent and vertically-ordered communities correspond to breaks in tidal flooding as quantified by tidal datums (Bertness et al., 1992). The MHHW tidal datum approximates the boundary between communities of C_4 plants on the high salt marsh and C_3 plants in the higher and less-frequently inundated brackish transitional zone (Bertness and Ellison, 1987; Johnson and York, 1915; Miller and Egler, 1950). The vertical zonation of salt-marsh plants (and specifically the narrow vertical range of the high salt-marsh platform occupied by C_4 plants) in Boston Harbor was recognized by historic workers. For example, a 1903 CE letter to the civil engineer J.R. Freeman from the surveyor J. Herbert Shedd (available upon request from author) describes how the salt-marsh surface was accepted to be a plane corresponding to mean high water and that even slight changes in elevation could be recognized by changes in vegetation; surveyors used this "marsh datum" for convenience. Furthermore, J.R. Freeman testified in a 1909 CE court case about ownership of Noddles Island in Boston Harbor that the salt-marsh surface "*is remarkably persistent at the plane of mean high water*".

We combined 50 new measurements of bulk sediment $\delta^{13}C$ from Belle Isle with existing datasets from Delaware to Rhode Island (Fig. 7). Standardization of Suess effect correction and tidal elevation facilitated direct comparison among sites (section 4.4). The relationship between elevation and $\delta^{13}C$ values is consistent across the study areas, with elevations above MHHW being characterized by $\delta^{13}C$ values more negative than −20‰ and locations below MHHW having $\delta^{13}C$ values less negative than −17‰. The isotopic difference between zones is relatively large and consistent among sites indicating that threshold values are applicable across sites experiencing different climate and ocean conditions today and are likely therefore to be robust through time. These values indicate that the in-situ plant community is a key source of organic carbon input to salt-marsh sediment. Samples that lie outside of the threshold values for elevation and isotopic composition may reflect spatially-variable (within and among sites) input of allochthonous organic carbon and in particular the transport of plant material across the narrow (meter-scale) MHHW boundary from one plant zone into another, for example during storms or particularly large astronomical tides and through bioturbation. Furthermore, collection of modern samples at and close to the upper boundary of salt marshes under conditions of RSL rise is likely to capture an active and dynamic environmental transition (Fagherazzi et al., 2019). In these circumstances, 1-cm thick sediment samples may contain (to varying degrees) plant material from both zones. The degree of confidence in threshold values could be changed by adjusting the boundary to be slightly below MHHW for isotopic values indicative of a botanical zone dominated by C_3 plants and slightly above MHHW for communities identified as being dominated by C_4 plants. The isotopic thresholds could also be revised. For example, there are 71 samples with $\delta^{13}C$ values more negative than −20‰, of which 52 (73%) were collected above MHHW. If the cut-off value is changed from −20‰ to −21/-22/-23‰ then the number of samples meeting this criteria in the dataset decreases, but the percentage of those samples occurring above MHHW increases to 76/80/83%, which suggests correspondingly higher confidence in setting informative priors for the BTF.

5.3. Late Holocene relative sea-level change

Trends in RSL at Belle Isle were estimated (95% credible intervals) through application of the NI-GAM (Upton et al., 2024) to a dataset of proxy reconstructions from Newfoundland to southern Florida, including the new dataset from Belle Isle. The long-term trend of RSL rise at ~1 mm/yr is consistent with the estimated contribution from GIA (Fig. 9B; Piecuch et al., 2018). The most prominent feature of the RSL reconstruction is the historic acceleration in the rate of rise to reach 2.98 mm/yr (2.46–3.51 mm/yr 95% credible interval) in 2017 CE. Using water-level measurements recovered in documentary archives, Talke et al. (2018) extended the Boston tide-gauge record to 1832 CE and identified an increase in the rate of RSL rise at 1919–1932 CE, which is also inferred from analyses of global tide-gauge records (Church and White, 2011; Dangendorf et al., 2017; Hay et al., 2015). Input to the NI-GAM did not include any tide-gauge data, therefore this result demonstrates that individual salt marshes can accurately record the observed acceleration of RSL rise. Accelerated RSL rise can be recorded in two ways by salt marshes; a reduction in paleomarsh elevation (i.e., drowning) as quantified by the BTF and through faster sediment accumulation. Early in the 20th century (~22 cm in core 201, estimated by

the age depth model to be ~1925 CE; Fig. 3) assemblages of foraminifera comprised almost entirely of high salt-marsh taxa transition abruptly to assemblages with increased abundance of *Miliammina fusca*, which is characteristic of lower elevations (Fig. 8). The age-depth model (Fig. 3) indicates higher sedimentation rates too, which is consistent with our inference (Fig. 5) that faster accumulation rates are readily detectable in radiocarbon-dated salt-marsh stratigraphies. The abrupt change in the proxy (foraminifera) record is less sharp in the NI-GAM (Fig. 9A, inset) because the vertical uncertainty of the underlying reconstruction (±25 cm since 1800 CE) is large compared to the amount of RSL change measured by the Boston tide gauge (~0.29 m).

While accelerating rates of RSL rise globally are quantitatively attributed to contemporary warming and specifically steric changes with more recent increases in ocean mass (Frederikse et al., 2020), historic correspondence suggests that this trend was observed by workers in the early 20th century. J.R. Freeman compiled water-level measurements from Boston and New York City and used those observations to suggest that coastal subsidence was occurring (Talke et al., 2018). Testifying in a 1903 CE court case about land ownership boundaries and tidal datums, Freeman commented that the rate of subsidence appeared to increase in the late 19th or early 20th century. Although this rate change was challenging to explain through known mechanisms of subsidence, he postulated that "*making a different amount of water in the form of ice*" was a possibility. The RSL reconstruction from Belle Isle with others from New York City (Kemp et al., 2017) and the Atlantic coast of North America (Gehrels et al., 2020; Kemp et al., 2018; Walker et al., 2021) suggests that the increased rate of subsidence inferred by Freeman was likely ongoing GIA (long-term RSL rise) compounded not by faster (or a new cause of) subsidence, but rather by sea-level rise through thermal expansion and increased ocean mass. However, Freeman was perhaps the first worker to document (during his own lifetime) the onset of modern, accelerated sea-level rise that is now recognized as a global phenomenon.

The NI-GAM decomposes the total RSL signal at sites in a network of reconstructions into categories that represent contributions from physical processes operating on particular spatial and temporal scales, rather than specific mechanisms (Fig. 10). The local-linear term describes processes that vary in rate among sites, but contributed at a constant rate through time. At Belle Isle the linear trend was ~1 mm/yr, which is predominantly caused by GIA (Engelhart et al., 2009; Peltier, 1996; Piecuch et al., 2018), although on a timescale of ~4000 years there is likely a non-linear contribution from GIA. Since the NI-GAM did not analyze reconstructions beyond the Atlantic coast of North America, the signal that is common to all sites, may not represent global mean sea level (Upton et al., 2024) and is hence termed 'regional non-linear' (Fig. 11). During the pre-industrial Common Era, this term displayed multi-century variability around 0 mm/yr. Processed-based modeling suggests that this variability primarily occurred in response to changing ocean temperature and glacier mass balance (particularly those in Arctic Canada and Russia and the periphery of Greenland) because changes in ocean mass caused by melt or growth of ice sheets in Greenland and Antarctica likely canceled one another out (Gangadharan et al., 2022). The rate of change increased sharply to reach 1.56 mm/yr (1.10–2.03 mm/yr; 95% credible interval) in 2017 CE, which is consistent with century-scale global mean sea-level rise estimated by analysis of proxy reconstructions (Kopp et al., 2016) and tide-gauge records (Dangendorf et al., 2017; Frederikse et al., 2020; Hay et al., 2015). The local, non-linear trend in the NI-GAM decomposition is site specific. At Belle Isle this term varied on multi-century timescales and remained close to 0 mm/yr, but prior to approximately −1200 CE the mean rate was negative (Fig. 10). This could reflect a local disequilibrium between the Belle Isle salt marsh and RSL at the time when decelerating global sea-level rise enabled salt marshes to establish (Horton et al., 2018; Peltier, 1996), or a more geographically coherent signal, but there are

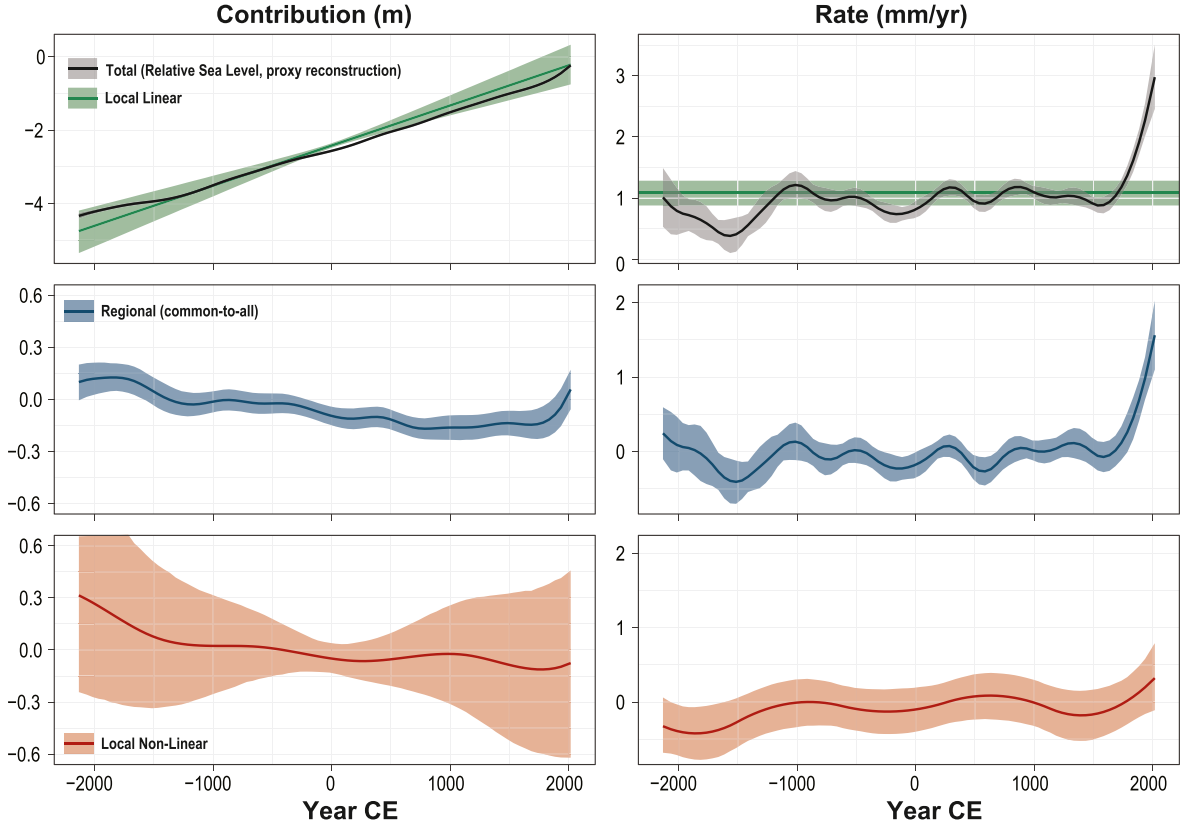

Fig. 10. Decomposition of RSL trends at Belle Isle along the Atlantic coast of North America from the noisy input generalized additive model (NI-GAM). Left column is the contribution and right column is the rate. Envelopes represent the 95% posterior interval at 50-year timesteps.

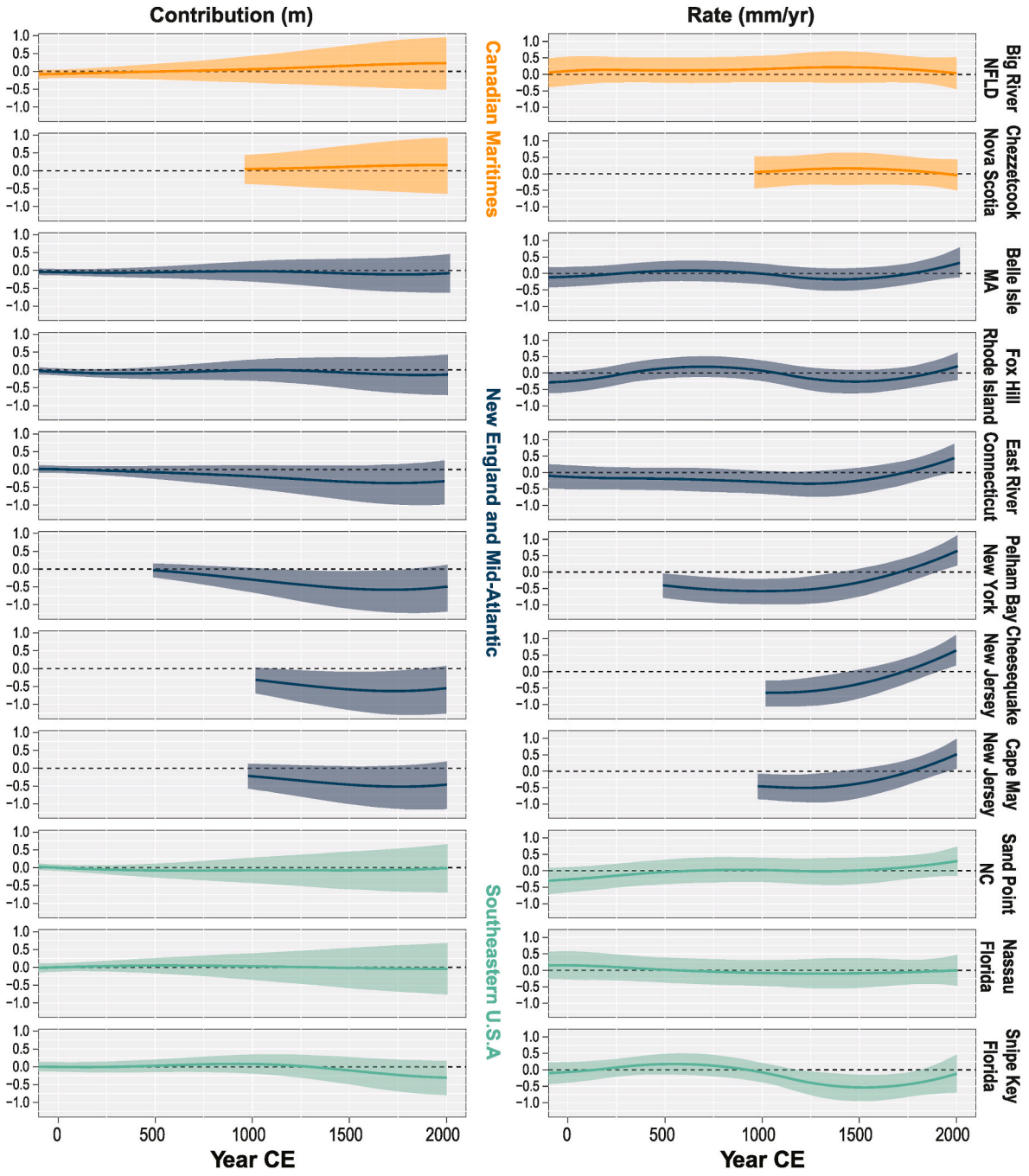

Fig. 11. Local non-linear sea-level trends estimated by the noisy input generalized additive model (NI-GAM) for sites along the Atlantic coast of North America (ordered from north, top, to south, bottom). Left column is the contribution and right column is the rate. Envelopes represent the 95% posterior interval at 50-year timesteps. Sites are colored to reflect geographic division into oceanographic regions.

few near-continuous RSL reconstructions which extend to −1500 CE. The decomposed RSL signal at Snipe Key in southern Florida (Khan et al., 2022) does not include this negative local, non-linear rate. Since ~1750 CE the local non-linear signal at Belle Isle occurred at a positive rate, although the 95% credible interval does include 0 mm/yr (Fig. 10). This feature is present in decomposed sea-level trends from Massachusetts to North Carolina, but appears absent in the southeastern United States and Canadian Maritimes. Sallenger et al. (2012) analyzed tide-gauge records along the Atlantic coast of North America and identified a hotspot of 20th century sea-level rise from Cape Hatteras (North Carolina) to Boston when calculating trends over a 60-year window, which was posited to result from dynamic processes. The temporal averaging and uncertainty (vertical and temporal) that is inherent with salt-marsh RSL reconstructions, caused the NI-GAM to recognize a smoother transition to modern rates of rise at Belle Isle (Fig. 9A inset), although the mid-points of the reconstruction indicated a more abrupt change. Therefore, the positive non-linear signal on the mid-Atlantic coast since ~1750 CE could reflect physical and statistical smoothing, or the initiation of a hotspot prior to tide gauges being established.

6. Conclusions

We generated a proxy-based RSL reconstruction spanning the past ~4200 years for Boston Harbor, during which RSL rose by ~4.2 m. A

Bayesian transfer function analyzed assemblages of foraminifera preserved in a core of salt-marsh sediment to estimate the elevation of past RSL and utilized informative prior information from bulk-sediment $\delta^{13}C$ values. A history of sediment accumulation constrained by 87 radiocarbon ages (at 58 unique depths) and recognition of three horizons of known age (including the sedimentary signature of Logan airport's expansion) was the basis for estimating sample age. This unusually high density of radiocarbon dates was used to test the sensitivity of age-depth models from salt-marsh sediment to necessary choices about the preparation, number, and distribution of plant macrofossils in core material. We show that common salt-marsh plant macrofossils (such as the rhizomes of *Spartina patens* and *Distichlis spicata*) can be prepared for radiocarbon dating through manual washing (no chemical pretreatment) and that there is little difference in reported ages (and their uncertainties) from traditional and single-step graphitization. The precision of age-depth models improves as more radiocarbon dates are available, but with diminishing returns. Periods of faster sedimentation are recognized with a relatively low density of radiocarbon dates, while a relatively high density is necessary to reliably identify slower sedimentation. RSL changes in Boston Harbor during the past ~4200 years reflect GIA overprinted by basin-scale processes. Sea-level variability among sites and sub-regions on the Atlantic coast of North America was likely modest, although the mid-Atlantic region shows faster rates of rise than the southeastern United States and Canadian Maritimes since ~1750 CE. The most pronounced feature is the onset of historic rates of rise, which is the fastest rate of rise in at least four millennia. This change in rate is recorded by the proxy RSL reconstruction from salt-marsh sediment, historic water-level measurements and may have been identified by workers in the early 20th century.

CRediT authorship contribution statement

Andrew C. Kemp: Conceptualization, Data curation, Formal analysis, Funding acquisition, Investigation, Methodology, Project administration, Supervision, Visualization, Writing – original draft, Writing – review & editing. **Elaine M. Whetstine:** Data curation, Formal analysis, Writing – original draft. **John C. Ridge:** Conceptualization, Investigation, Supervision, Writing – review & editing.

Declaration of competing interest

The authors declare that they have no known competing financial interests or personal relationships that could have appeared to influence the work reported in this paper.

The author is an Editorial Board Member/Editor-in-Chief/Associate Editor/Guest Editor for *[Journal name]* and was not involved in the editorial review or the decision to publish this article.

The authors declare the following financial interests/personal relationships which may be considered as potential competing interests:

Acknowledgements

Jack Ridge proposed working at Belle Isle having taken students coring at the site for many years. We are grateful for help in the field and lab from Dr. Juliet Sefton, Dr. Emmanuel Bustamante, and Tufts undergraduates Caroline Gleason, Jacob Marsh, and Ella Erskine. Prof. Jon Woodruff (UMass Amherst) facilitated access to the ITRAX core scanner. The R code for resampling of radiocarbon dates was written with considerable assistance from Uku-Kasper Uustalu (Tufts University, Data Science). We thank Kathy Elder at NOSAMS for her ongoing help with all things radiocarbon. Plot colors are inspired by historic British Rail liveries. This work was supported by NSF awards OCE-2002431 and OCE-1942563 and is a contribution to IGCP project 725 (Forecasting Coastal Change). We are grateful to two anonymous reviewers for providing their time and expertise to improve this paper.

Appendix A. Supplementary data

Supplementary data to this article can be found online at https://doi.org/10.1016/j.quascirev.2024.109053.

Data availability

Data provided as supporting files

References

Bertness, M.D., Ellison, A.M., 1987. Determinants of pattern in a new England salt marsh plant community. Ecol. Monogr. 57, 129–147.
Bertness, M.D., Wikler, K., Chatkupt, T., 1992. Flood tolerance and the distribution of Iva frutescens across New England salt marshes. Oecologia 91, 171–178.
Brock, F., Higham, T., Ditchfield, P., Ramsey, C.B., 2010. Current pretreatment methods for AMS radiocarbon dating at the oxford radiocarbon accelerator unit (orau). Radiocarbon 52, 103–112.
Cahill, N., Kemp, A.C., Parnell, A.C., Horton, B.P., 2016. A Bayesian hierarchical model for reconstructing relative sea level: from raw data to rates. Clim. Past 12, 525–542.
Chmura, G.L., Aharon, P., 1995. Stable carbon isotope signatures of sedimentary carbon in coastal wetlands as indicators of salinity regime. J. Coast Res. 11, 124–135.
Church, J.A., White, N.J., 2011. Sea-level rise from the late 19th to the early 21st century. Surv. Geophys. 32, 585–602.
Corbett, D.R., Walsh, J.P., 2015. ^{210}Lead and ^{137}Cesium: establishing a chronology for the last century. In: Shennan, I., Long, A.J., Horton, B.P. (Eds.), Handbook of Sea Level Research. John Wiley & Sons, Chichester, pp. 361–372.
Dangendorf, S., Marcos, M., Wöppelmann, G., Conrad, C.P., Frederikse, T., Riva, R., 2017. Reassessment of 20th century global mean sea level rise. In: Proceedings of the National Academy of Sciences, vol. 114, pp. 5946–5951.
de Rijk, S., 1995a. Agglutinated foraminifera as indicators of salt marsh development in relation to late Holocene sea level rise. Febo, Utrecht 188.
de Rijk, S., 1995b. Salinity control on the distribution of salt marsh foraminifera (Great Marshes, Massachusetts). J. Foraminifer. Res. 25, 156–166.
de Rijk, S., Troelstra, S.R., 1997. Salt marsh foraminifera from the Great Marshes, Massachusetts: environmental controls. Palaeogeogr. Palaeoclimatol. Palaeoecol. 130, 81–112.
DeConto, R., FitzGerald, D., Hay, C., Hughes, Z., Kemp, A.C., Kopp, R.E., 2016. Sea-level rise. In: Boston, C.R. (Ed.), Climate ready Boston: Climate Change and Sea-Level Rise Projections for Boston. University of Massachusetts, Boston, p. 54.
DeGroot, D.J., Landon, M.E., Poirier, S.E., 2019. Geology and engineering properties of sensitive Boston blue clay at newbury, Massachusetts. AIMS Geosciences 5, 412–447.
Dunnington, D.W., Roberts, S., Norton, S.A., Spooner, I.S., Kurek, J., Kirk, J.L., Muir, D.C. G., White, C.E., Gagnon, G.A., 2020. The distribution and transport of lead over two centuries as recorded by lake sediments from northeastern North America. Sci. Total Environ. 737, 140212.
Edwards, R.J., Wright, A.J., 2015. Foraminifera. In: Shennan, I., Long, A.J., Horton, B.P. (Eds.), Handbook of Sea-Level Research. John Wiley & Sons, Chichester, pp. 191–217.
Edwards, R.J., Wright, A.J., van de Plassche, O., 2004. Surface distributions of salt-marsh foraminifera from Connecticut, USA: modern analogues for high-resolution sea level studies. Mar. Micropaleontol. 51, 1–21.
Elder, K.L., Roberts, M.L., Walther, T., Xu, L., 2019. Single step production of graphite from organic samples for radiocarbon measurements. Radiocarbon 61, 1843–1854.
Eleuterius, L., 1976. The distribution of *Juncus roemerianus* in the salt marshes of North America. Chesap. Sci. 17, 289–292.
Engelhart, S.E., Horton, B.P., Douglas, B.C., Peltier, W.R., Tornqvist, T.E., 2009. Spatial variability of late Holocene and 20th century sea-level rise along the Atlantic coast of the United States. Geology 37, 1115–1118.
Fagherazzi, S., Anisfeld, S.C., Blum, L.K., Long, E.V., Feagin, R.A., Fernandes, A., Kearney, W.S., Williams, K., 2019. Sea level rise and the dynamics of the marsh-upland boundary. Front. Environ. Sci. 7.
Filipescu, S., Kaminski, M.A., 2008. Re-discovering *Entzia*, an agglutinated foraminifer from the Transylvanian salt marshes. In: Filipescu, S., Kaminski, M.A. (Eds.), Eigth International Workshop on Agglutinated Foraminifera. The Grzybowski Foundation, Cluj-Napoca, Romania, pp. 29–35.
Frederikse, T., Landerer, F., Caron, L., Adhikari, S., Parkes, D., Humphrey, V.W., Dangendorf, S., Hogarth, P., Zanna, L., Cheng, L., Wu, Y.-H., 2020. The causes of sea-level rise since 1900. Nature 584, 393–397.
Gangadharan, N., Goosse, H., Parkes, D., Goelzer, H., Maussion, F., Marzeion, B., 2022. Process-based estimate of global-mean sea-level changes in the Common Era. Earth Syst. Dynam. 13, 1417–1435.
Gehrels, W.R., 2000. Using foraminiferal transfer functions to produce high-resolution sea-level records from salt-marsh deposits, Maine, USA. Holocene 10, 367–376.
Gehrels, W.R., van de Plassche, O., 1999. The use of *Jadammina macrescens* (brady) and *Balticammina pseudomacrescens* brönnimann, lutze and whittaker (Protozoa: Foraminiferida) as sea-level indicators. Palaeogeogr. Palaeoclimatol. Palaeoecol. 149, 89–101.
Gehrels, W.R., Kirby, J.R., Prokoph, A., Newnham, R.M., Achterberg, E.P., Evans, H., Black, S., Scott, D.B., 2005. Onset of recent rapid sea-level rise in the western Atlantic Ocean. Quat. Sci. Rev. 24, 2083–2100.

Gehrels, W.R., Dangendorf, S., Barlow, N., Saher, M., Long, A., Woodworth, P., Piecuch, C., Berk, K., 2020. A preindustrial sea-level rise hotspot along the Atlantic coast of North America. Geophys. Res. Lett. 47 e2019GL085814.
Hawkes, A.D., Horton, B.P., Nelson, A.R., Hill, D.F., 2010. The application of intertidal foraminifera to reconstruct coastal subsidence during the giant Cascadia earthquake of AD 1700 in Oregon, USA. Quat. Int. 221, 116–140.
Hay, C., Morrow, E., Kopp, R.E., Mitrovica, J.X., 2015. Probabilistic reanalysis of twentieth-century sea-level rise. Nature 517, 481–484.
Hill, T.D., Anisfeld, S.C., 2021. VulnToolkit: Analysis of Tidal Datasets, 1.1.4 ed.
Holgate, S.J., Matthews, A., Woodworth, P.L., Rickards, L.J., Tamisiea, M.E., Bradshaw, E., Foden, P.R., Gordon, K.M., Jevrejeva, S., Pugh, J., 2013. New data systems and products at the permanent service for mean Sea Level. J. Coast Res. 29, 493–504.
Horton, B.P., Edwards, R.J., 2006. Quantifying Holocene Sea-Level Change Using Intertidal Foraminifera: Lessons from the British Isles. Cushman Foundation for Foraminiferal Research, Washington D.C.
Horton, B.P., Shennan, I., Bradley, S.L., Cahill, N., Kirwan, M., Kopp, R.E., Shaw, T.A., 2018. Predicting marsh vulnerability to sea-level rise using Holocene relative sea-level data. Nat. Commun. 9, 2687.
Johnson, D.S., York, H.H., 1915. The Relation of Plants to Tide-Levels; a Study of Factors Affecting the Distribution of Marine Plants. Carnegie Institution of, Washington, Washington, D.C.
Keeling, C.D., 1979. The Suess effect: ^{13}Carbon-^{14}Carbon interrelations. Environ. Int. 2, 229–300.
Kemp, A.C., Vane, C.H., Horton, B.P., Engelhart, S.E., Nikitina, D., 2012. Application of stable carbon isotopes for reconstructing salt-marsh floral zones and relative sea level, New Jersey, USA. J. Quat. Sci. 27, 404–414.
Kemp, A.C., Nelson, A.R., Horton, B.P., 2013. Radiocarbon dating of plant macrofossils in tidal marsh sediment. In: Schroder, J. (Ed.), Treatise on Geomorphology. Academic Press, San Diego, CA, pp. 370–388.
Kemp, A.C., Hill, T.D., Vane, C.H., Cahill, N., Orton, P., Talke, S.A., Parnell, A.C., Sanborn, K., Hartig, E.K., 2017. Relative sea-level trends in New York City during the past 1500 years. Holocene 27, 1169–1186.
Kemp, A.C., Wright, A.J., Edwards, R.J.B.R.L., Brain, M., Cahill, N., Kopp, R.E., Horton, B.P., Charman, D.J., Hawkes, A.D., Hill, T.D., van de Plassche, O., 2018. Relative sea-level change in Newfoundland, Canada during the past ~3000 years. Quat. Sci. Rev. 201, 89–110.
Kemp, A.C., Wright, A.J., Cahill, N., 2020. Enough is enough, or more is more? Testing the influence of foraminiferal count size on reconstructions of paleo-marsh elevation. J. Foraminifer. Res. 50, 266–278.
Khan, N.S., Ashe, E., Moyer, R.P., Kemp, A.C., Engelhart, S.E., Brain, M.J., Toth, L.T., Chappel, A., Christie, M., Kopp, R.E., Horton, B.P., 2022. Relative sea-level change in South Florida during the past ~5000 years. Global Planet. Change 216, 103902.
Kopp, R.E., Kemp, A.C., Bitterman, K., Horton, B.P., Donnelly, J.P., Gehrels, W.R., Hay, C., Mitrovica, J.X., Morrow, E., Rahmstorf, S., 2016. Temperature-driven global sea-level variability in the Common Era. In: Proceedings of the National Academy of Sciences, vol. 113, pp. E1434–E1441.
Kwon, E.Y., Timmermann, A., Tipple, B.J., Schmittner, A., 2022. Projected reversal of oceanic stable carbon isotope ratio depth gradient with continued anthropogenic carbon emissions. Communications Earth & Environment 3, 62.
Lacourse, T., Gajewski, K., 2020. Current practices in building and reporting age-depth models. Quaternary Research 96, 28–38.
Lamb, A.L., Wilson, G.P., Leng, M.J., 2006. A review of coastal palaeoclimate and relative sea-level reconstructions using δ^{13}C and C/N ratios in organic material. Earth Sci. Rev. 75, 29–57.
Lima, A.L., Bergquist, B.A., Boyle, E.A., Reuer, M.K., Dudas, F.O., Reddy, C.M., Eglinton, T.I., 2005. High-resolution historical records from Pettaquamscutt River basin sediments: 2. Pb isotopes reveal a potential new stratigraphic marker. Geochem. Cosmochim. Acta 69, 1813–1824.
Marshall, W., 2015. Chronohorizons: indirect and unique event dating methods for sea-level reconstructions. In: Shennan, I., Long, A.J., Horton, B.P. (Eds.), Handbook of Sea-Level Research. Wiley, pp. 373–385.
Martello, M.V., Whittle, A.J., 2023. Estimating coastal flood damage costs to transit infrastructure under future sea level rise. Communications Earth & Environment 4, 137.
Miller, W.R., Egler, F.E., 1950. Vegetation of the wequetequock-pawcatuck tidal-marshes, Connecticut. Ecol. Monogr. 20, 143–172.
Niering, W.A., Warren, R.S., Weymouth, C.G., 1977. Our dynamic tidal marshes: vegetation changes as revealed by peat analysis. In: The Connecticut Arboretum Bulletin, vol. 22, p. 12.
Norris, M.W., Turnbull, J.C., Howarth, J.D., Vandergoes, M.J., 2020. Pretreatment of terrestrial macrofossils. Radiocarbon 62, 349–360.
Parnell, A.C., Gehrels, W.R., 2015. Using chronological models in late Holocene sea-level reconstructions from saltmarsh sediments. In: Shennan, I., Long, A.J., Horton, B.P. (Eds.), Handbook of Sea-Level Research. John Wiley & Sons, pp. 500–513.
Parnell, A.C., Haslett, J., Allen, J.R.M., Buck, C.E., Huntley, B., 2008. A flexible approach to assessing synchroneity of past events using Bayesian reconstructions of sedimentation history. Quat. Sci. Rev. 27, 1872–1885.
Parnell, A.C., Buck, C.E., Doan, T.K., 2011. A review of statistical chronology models for high-resolution, proxy-based Holocene palaeoenvironmental reconstruction. Quat. Sci. Rev. 30, 2948–2960.
Parsons, T., Wu, P.-C., Wei, M., D'Hondt, S., 2023. The weight of New York City: possible contributions to subsidence from anthropogenic sources. Earth's Future 11, e2022EF003465.
Peltier, W.R., 1996. Global sea level rise and glacial isostatic adjustment: an analysis of data from the east coast of North America. Geophys. Res. Lett. 23, GL00848.
Piecuch, C.G., Huybers, P., Hay, C.C., Kemp, A.C., Little, C.M., Mitrovica, J.X., Ponte, R. M., Tingley, M.P., 2018. Origin of spatial variation in US East Coast sea-level trends during 1900–2017. Nature 564, 400–404.
Ray, R.D., Foster, G., 2016. Future nuisance flooding at Boston caused by astronomical tides alone. Earth's Future 4, 578–587.
Redfield, A.C., 1972. Development of a new England salt marsh. Ecol. Monogr. 42, 201–237.
Reimer, P.J., Austin, W.E., Bard, E., Bayliss, A., Blackwell, P.G., Ramsey, C.B., Butzin, M., Cheng, H., Edwards, R.L., Friedrich, M., 2020. The IntCal20 Northern Hemisphere radiocarbon age calibration curve (0–55 cal kBP). Radiocarbon 62, 725–757.
Rousseeuw, P., 1987. Silhouettes: a graphical aid to the interpretation and validation of cluster techniques. J. Comput. Appl. Math. 20, 53–65.
Sallenger, A.H., Doran, K.S., Howd, P.A., 2012. Hotspot of accelerated sea-level rise on the Atlantic coast of North America. Nat. Clim. Change 2, 884–888.
Scott, D.B., Medioli, F.S., 1978. Vertical zonations of marsh foraminifera as accurate indicators of former sea levels. Nature 272, 528–531.
Scott, D.B., Medioli, F.S., 1980. Quantitative Studies of Marsh Foraminiferal Distributions in Nova Scotia: Implications for Sea Level Studies, vol. 17. Cushman Foundation for Foraminiferal Research.
Seasholes, N.S., 2018. Gaining Ground: A History of Landmaking in Boston. MIT Press, Cambridge, MA.
Sefton, J., Kemp, A.C., Elder, K.L., Hansman, R., Roberts, M.L., 2022a. Implications of single-step graphitization for reconstructing late Holocene relative sea-level using radiocarbon-dated organic coastal sediment. Radiocarbon 64, 1139–1158.
Sefton, J.P., Kemp, A.C., Elder, K.L., Hansman, R.L., Roberts, M.L., 2022b. Implications of single-step graphitization for reconstructing late Holocene realtive sea level using radiocarbon-dated organic coastal sediment. Radiocarbon 64, 1139–1158.
Simpson, G.L., 2007. Analogue methods in palaeoecology: using the analogue package. J. Stat. Software 22, 1–29.
Stearns, R.B., Engelhart, S.E., Kemp, A.C., Hill, T.D., Brain, M.J., Corbett, D.R., 2023. Within-region replication of late Holocene relative sea-level change: an example from southern New England, United States. Quat. Sci. Rev. 300, 107868.
Strauss, B.H., Kulp, S., Levermann, A., 2015. Carbon choices determine US cities committed to futures below sea level. In: Proceedings of the National Academy of Sciences, vol. 112, pp. 13508–13513.
Stuiver, M., Polach, H.A., 1977. Reporting of ^{14}C data. Radiocarbon 19, 355–363.
Swindles, G.T., Outram, Z., Batt, C.M., Hamilton, W.D., Church, M.J., Bond, J.M., Watson, E.J., Cook, G.T., Sim, T.G., Newton, A.J., Dugmore, A.J., 2019. Vikings, peat formation and settlement abandonment: a multi-method chronological approach from Shetland. Quat. Sci. Rev. 210, 211–225.
Synal, H.-A., Stocker, M., Suter, M., 2007. MICADAS: a new compact radiocarbon AMS system. Nucl. Instrum. Methods Phys. Res. Sect. B Beam Interact. Mater. Atoms 259, 7–13.
Talke, S.A., Kemp, A.C., Woodruff, J.D., 2018. Realtive sea level, tides, and extreme water levels in Boston Harbor from 1825 to 2018. J. Geophys. Res.: Oceans 123, 3895–3914.
Upton, M., Parnell, A.C., Kemp, A.C., Ashe, E., McCarthy, G., Cahill, N., 2024. A Noisy-Input Generalised Additive Model for Relative Sea-Level Change along the Atlantic Coast of North America, qlae044. Royal Statistical Society: Series C.
van de Plassche, O., 1991. Late Holocene sea-level fluctuations on the shore of Connecticut inferred from transgressive and regressive overlap boundaries in salt-marsh deposits. J. Coast Res. 11, 159–179.
Walker, J.S., Kopp, R.E., Shaw, T.A., Cahill, N., Khan, N.S., Barber, D.C., Ashe, E.L., Brain, M.J., Clear, J.L., Corbett, D.R., Horton, B.P., 2021. Common Era sea-level budgets along the U.S. Atlantic coast. Nat. Commun. 12, 1841.
Walker, J.S., Kopp, R.E., Little, C.M., Horton, B.P., 2022. Timing of emergence of modern rates of sea-level rise by 1863. Nat. Commun. 13, 966.
Walton, W.R., 1952. Techniques for recognition of living foraminifera. Cushman Foundation for Foraminiferal Research 3, 56–60.
Waters, C.N., Turner, S.D., 2022. Defining the onset of the anthropocene. Science 378, 706–708.
Williams, S., Garrett, E., Moss, P., Bartlett, R., Gehrels, W.R., 2021. Development of a training set of contemporary salt-marsh foraminifera for late Holocene sea-level reconstructions in southeastern Australia. Open Quat. 7, 4.
Wilson, G.P., 2017. On the application of contemporary bulk sediment organic carbon isotope and geochemical datasets for Holocene sea-level reconstruction in NW Europe. Geochem. Cosmochim. Acta 214, 191–208.
Wilson, G.P., Lloyd, J., Khan, N.S., Kemp, A.C., 2024. Developments in the application of stable carbon isotopes and bulk geochemistry as indicators of relative sea-level change in tidal wetlands and isolation basins. Quat. Sci. Rev. 340, 108855.
Woodroffe, S., Barlow, N.L.M., 2015. Reference water level and tidal datum. In: Shennan, I., Long, A.J., Horton, B.P. (Eds.), Handbook of Sea-Level Research. John Wiley & Sons, Chichester, pp. 171–182.
Wright, A.J., Edwards, R.J., van de Plassche, O., Blaauw, M., Parnell, A.C., van der Borg, K., de Jong, A.F., Roe, H.M., Selby, K., Black, S., 2017. Reconstructing the accumulation history of a saltmarsh sediment core: which age-depth model is best? Quat. Geochronol. 39, 35–67.
Yang, Z., Myers, E., Jeong, S., White, S., 2013. VDatum for the Gulf of Maine:Tidal Datums and Topography of the Sea Surface. Technical Memorandum. NOAA, p. 50.